Longitudinal plasma proteomics analysis reveals novel candidate biomarkers in acute COVID-19

Mohammed, Y.; Goodlett, D.R.; Cheng, M.P.; Vinh, D.C.; Lee, T.C.; Mcgeer, A.; ... ; ARBs CORONA I

Journal of proteome research

pubs.acs.org/jpr

Article

Longitudinal Plasma Proteomics Analysis Reveals Novel Candidate Biomarkers in Acute COVID-19

Yassene Mohammed,* David R. Goodlett, Matthew P. Cheng, Donald C. Vinh, Todd C. Lee, Allison Mcgeer, David Sweet, Karen Tran, Terry Lee, Srinivas Murthy, John H. Boyd, Joel Singer, Keith R. Walley, David M. Patrick, Curtis Quan, Sara Ismail, Laetitia Amar, Aditya Pal, Rayhaan Bassawon, Lara Fesdekjian, Karine Gou, Francois Lamontagne, John Marshall, Greg Haljan, Robert Fowler, Brent W. Winston, James A. Russell,* and ARBs CORONA I

Cite This: *J. Proteome Res.* 2022, 21, 975−992

Read Online

ACCESS | Metrics & More | Article Recommendations | Supporting Information

ABSTRACT: The host response to COVID-19 pathophysiology over the first few days of infection remains largely unclear, especially the mechanisms in the blood compartment. We report on a longitudinal proteomic analysis of acute-phase COVID-19 patients, for which we used blood plasma, multiple reaction monitoring with internal standards, and data-independent acquisition. We measured samples on admission for 49 patients, of which 21 had additional samples on days 2, 4, 7, and 14 after admission. We also measured 30 externally obtained samples from healthy individuals for comparison at baseline. The 31 proteins differentiated in abundance between acute COVID-19 patients and healthy controls belonged to acute inflammatory response, complement activation, regulation of inflammatory response, and regulation of protein activation cascade. The longitudinal analysis showed distinct profiles revealing increased levels of multiple lipid-associated functions, a rapid decrease followed by recovery for complement activation, humoral immune response, and acute inflammatory response-related proteins, and level fluctuation in the regulation of smooth muscle cell proliferation, secretory mechanisms, and platelet degranulation. Three proteins were differentiated between survivors and nonsurvivors. Finally, increased levels of fructose−bisphosphate aldolase B were determined in patients with exposure to angiotensin receptor blockers versus decreased levels in those exposed to angiotensin-converting enzyme inhibitors. Data are available via ProteomeXchange PXD029437.

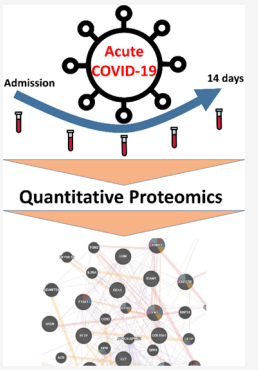

KEYWORDS: *COVID-19, targeted quantitative proteomics, amyloid, complement, ARB, ACEi, longitudinal analysis*

INTRODUCTION

The COVID-19 pandemic continues to grow and affect human health and the world economy in many ways. COVID-19 disease, which is promoted by SARS-CoV-2 viral infection, induces a variable spectrum of symptoms such as fever, cough, dyspnea, chills, muscle pain, and loss of taste or smell. Severe disease is worse in males and older patients, with the exact mechanisms still not fully understood, requiring further study.[1−4] Cellular entry follows on from the interaction between the spike protein S of SARS-CoV-2 with the angiotensin-converting enzyme 2 (ACE2) receptor,[5−10] which is expressed in many human tissues and at a medium level in the upper and lower respiratory tract.[11] An average mortality rate of 17.1% was reported for patients admitted to hospitals, with 40.5% for patients in critical situation.[12]

COVID-19 continues to be the subject of many scientific reports that make use of various sample types and analytical methods. Bojkova et al.[13] used proteomics and the Orbitrap analyzer to study the pathways modulated by SARS-CoV-2 in the human cell culture model they developed. They found effects on pathways related to translation, splicing, carbon metabolism, protein homeostasis, and nucleic acid metabolism. Gordon et al.[14] used affinity purification−mass spectrometry and determined 332 protein−protein interactions between SARS-CoV-2 and human proteins. Their findings identified interactions with proteins belonging to various biological processes and complexes including DNA replication, epigenetic and gene expression regulators, vesicle trafficking, lipid modification, RNA processing and regulation, ubiquitin ligases, signaling, and nuclear transport machinery. Multiple innate immune pathways and host translation machinery were also among the pathways affected. Geyer et al.[15] performed a longitudinal proteomic analysis using data-dependent acquisition and a trapped ion mobility spectrometry time-of-flight instrument[16,17] on plasma samples from 31 COVID-19 hospitalized patients. They found innate immune system proteins decreased early in the time course while the regulators

Received: November 5, 2021
Published: February 10, 2022

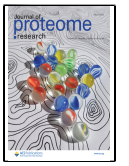

https://doi.org/10.1021/acs.jproteome.1c00863
J. Proteome Res. 2022, 21, 975−992

of coagulation and lipid homeostasis increased over time. Mun et al.[18] profiled the nasopharyngeal swabs of COVID-19 patients using a similar instrumental setup as Geyer et al.[15] but operated in the data-independent acquisition (DIA) mode. Their results revealed various alterations in the processes related to innate immune response and exocytosis.

Acute COVID-19 causes widespread changes in host immune, inflammatory, and coagulation responses that are potential biomarkers and therapeutic targets. However, to date, there has been limited investigation of the effects of acute COVID-19 on plasma proteomics during the first few weeks of hospitalization. One study[19] of 46 COVID-19 patients and 53 controls found 93 proteins that had differential expression in severe COVID-19. Whetton and colleagues[20] evaluated proteomics and used artificial intelligence to understand acute COVID-19 proteomics.

Our objective, therefore, was to investigate whether plasma protein abundances in COVID-19 patients measured using proteomic analysis differ from healthy controls and change over the course of two weeks after admission. We used plasma samples from 49 acute-phase COVID-19 patients and 30 externally obtained plasma samples from healthy individuals. The secondary aims were to determine whether there were differences in plasma protein levels in COVID-19 patients between males and females, survivors and nonsurvivors, and those who were or were not exposed to angiotensin receptor blockers (ARBs) and ACE inhibitors (ACEi). In a primary analysis, we used quantitative targeted proteomics with internal standards that allowed the quantification of multiple proteins in each sample. Additionally, having internal standards, spiked into all samples at the same level, allowed excellent comparability between samples. In parallel, we analyzed all samples using a DIA approach and compared both data sets.

MATERIALS AND METHODS

Ethics

This study was approved by the Providence Health Care and University of British Columbia Human Research Committee and by each of the contributing clinical sites. The anonymized clinical data and use of discarded plasma from clinical blood tests were deemed low risk, and informed consent was deemed not necessary for this research. This proteomic study was a substudy of ARBs and ACEi in adults hospitalized with acute COVID-19, ClinicalTrials.gov Identifier: NCT04510623.[21]

Patient Selection Criteria

Individuals over 18 years of age who had confirmed COVID-19 infection (according to local hospitals or provincial laboratories' clinically approved laboratory testing for SARS-CoV-2) who were admitted to hospitals were included. Patients who were admitted to hospitals for another reason who were SARS-CoV-2 positive were excluded. The plasma samples were collected using K_2EDTA tubes and processed within 4 h upon admission from 46 patients and on days 2, 4, 7, and 14. The control human plasma samples (n = 30) were obtained commercially from whole blood donors (Human Plasma K_2EDTA, BioIVT, Hicksville, NY, USA). The control subjects did not have COVID-19 and otherwise declared themselves to be healthy.

Baseline Characteristics of Healthy Controls and COVID-19 Patients

We recorded age and sex in the healthy controls and baseline (at study enrollment) characteristics in the COVID-19 patients [age, sex, and presence of heart failure, hypertension, chronic kidney disease, and diabetes (commonest comorbidities of 2019nCoV[22−24])] associated with the increased risk of intensive care unit (ICU) admission[24] and 28-day mortality.

Measurement of Plasma Using Targeted Quantitative Proteomics

We used targeted MS-based quantitative proteomic assays. The multiple reaction monitoring (MRM) assays were developed and validated at the University of Victoria Proteomics Centre, Victoria, BC, Canada,[25−29] and include internal standard peptides for 270 proteins. A list of the peptides and proteins is provided in Table S1. Although we target 270 proteins here, the panel typically quantifies between 160 and 175 proteins depending on the quality of the plasma samples and anticoagulant used.[30] In the current study, we were able to detect 192 proteins, of which 172 were quantified and used for further analysis.

Protein concentrations were determined by comparing their responses in the mass spectrometer with the responses of heavy labeled internal standard peptides spiked in the sample. The sample preparation protocol was developed previously[26,28] and is available from PeptideTracker.[27,29] Briefly, the sample digests were prepared through the denaturation and reduction of the homogenate with 9 M urea/20 mM dithiothreitol for 30 min at 37 °C. Denatured proteins were alkylated with iodoacetamide (40 mM final concentration) for 30 min at room temperature, and then samples were diluted to reach a final urea concentration of 0.55 mM prior to tryptic digestion. Digestion was carried out at a 10:1 substrate/enzyme ratio using tosyl phenylalanyl chloromethyl ketone-treated trypsin (Worthington) for 18 h at 37 °C. After digestion, the samples were acidified with aqueous 1% formic acid (FA), and a chilled, stable isotope-labeled standard peptide mixture was added. The samples were concentrated via solid phase extraction (SPE; 10 mg Oasis HLB cartridges; Waters), using the manufacturer's recommended protocol. The SPE column was conditioned with 100% methanol (1 mL), followed by washing with 100% H_2O/0.1% FA (1 mL). The sample (diluted to 1 mL using 100% H_2O/0.1% FA) was then loaded onto the column, followed by washing two times with water (1 mL each). Finally, the sample was eluted with 55% acetonitrile (can)/0.1% FA (300 μL) and lyophilized to dryness. The dried samples were rehydrated in 0.1% FA to a concentration of 1 μg/μL for liquid chromatography (LC)/MRM−MS analysis. The samples were separated on-line with a reversed phase-ultra-high-performance LC (RP-UHPLC) column (Eclipse Plus C18 RRHD 150 × 2.1 mm i.d., 1.8 μm particle diameter; Agilent) maintained at 50 °C. Peptide separations were performed at 0.4 mL/min over a 56 min run, via a multistep LC gradient. The solvents were aqueous mobile phase—solvent A—with 0.1% FA in LC−MS grade water, and the organic mobile phase—solvent B—with 0.1% FA in LC−MS grade acetonitrile. The exact gradient was as follows (time points in minutes, solution B %): 0 min, 2%; 2 min, 7%; 50 min, 30%; 53 min, 45%; 53.5 min, 80%; 55.5 min, 80%; and 56 min, 2%. A post-column equilibration of 4 min was used after each sample analysis. The LC system was interfaced to a triple quadrupole mass spectrometer (Agilent 6490) via a standard-

https://doi.org/10.1021/acs.jproteome.1c00863
J. Proteome Res. 2022, 21, 975−992

flow electrospray ionization source, operated in the positive ion mode. The MRM acquisition parameters employed for the quantitation were as follows: 3500 V capillary voltage, 300 V nozzle voltage, 11 L/min sheath gas flow at a temperature of 250 °C, 15 L/min drying gas flow at a temperature of 150 °C, 30 psi nebulizer gas pressure, 380 V fragmentor voltage, 5 V cell accelerator potential, and unit mass resolution in the first and third quadrupoles. For optimal peptide collision-induced dissociation, peptide-specific collision energy (CE) values had previously been determined experimentally. The exact CE values for each peptide is available from PeptideTracker.[27]

Measurement of Plasma Using DIA

With an estimated protein concentration of 70 μg/μL, 50 μg of each sample was denatured, reduced, alkylated, and digested using the Preomics iST sample preparation kit (Preomics GmbH, Martinsried, Germany). The samples were resuspended in load buffer at a concentration of 1 μg/μL and a DIA chromatogram library sample was created from a pooled aliquot of the samples. A 5 μL injection was separated by on-line reverse-phase chromatography using a Thermo Scientific EASY-nLC 1000 system with a reversed phase precolumn Magic C18-AQ (100 μm I.D., 2.5 cm length, 5 μm, 100 Å), and an in-house prepared reversed phase nano-analytical column Magic C-18AQ (75 μm I.D., 20 cm length, 5 μm, 100 Å, Michrom BioResources Inc., Auburn, CA), at a flow rate of 300 nL/min. The LC system was coupled on-line using an Orbitrap Fusion Tribrid mass spectrometer (Thermo Fisher Scientific, San Jose, CA) equipped with a Nanospray Flex NG source (Thermo Fisher Scientific). The LC aqueous mobile phase—solvent A was with 2% acetonitrile and 0.1% FA in LC−MS grade water, and the organic mobile phase—solvent B was with 0.1% FA in 90% acetonitrile samples were separated by a 64 min gradient with the following gradient (time points in minutes, solution B %): 0 min, 5% B; 50 min, 25% B; 52 min, 40% B; 54 min, 90% B; 59 min, 90% B; 60 min, 5% B; and 64 min, 5% B. The Orbitrap Fusion instrument parameters (Fusion Tune 3.3 software) were as follows for an Orbitrap (OT-MS) iontrap (OT-MS/MS) with HCD fragmentation: A nano-electrospray ion source with a spray voltage of 2.55 kV and a capillary temperature of 275 °C.

To create a chromatogram library, we acquired six chromatogram library acquisitions with a 60,000 resolution full MS1 spectrum matching the range (i.e., 395−505,495−605, 595−705, 695−805, 795−905, and 895−1005 m/z) using an AGC target of 4×10^5 and a maximum inject time of 60 ms. The MS2 acquisition strategy for DIA spectra was 4 m/z precursor isolation windows at 30,000 resolution, an AGC target of 4×10^5, a maximum inject time of 60 ms, charge state 3, HCD 33, and using an overlapping window pattern from narrow mass ranges using window placements optimized by EncyclopeDIA,[31] that is, 396.43−502.48, 496.48−602.52, 596.52−702.57, 696.57−802.61, 796.61−902.66, and 896.6−1002.70 m/z. For the sample measurement, the Orbitrap Fusion Tribrid was configured to acquire a 60,000 resolution full MS1 spectrum with 385−1015mz range, an AGC target of 4×10^5, a maximum inject time of 60 ms, and matching the range 25 × 24 m/z of DIA spectra (24 m/z precursor isolation windows at 30,000 resolution, an AGC target of 4×10^5, a maximum inject time of 60 ms, Charge state 3, and HCD 33) using an overlapping window pattern from 388.43 to 1012.70 m/z using window placements optimized by EncyclopeDIA.[31]

Data Processing

MRM Data Processing. Skyline was used to inspect the peptide response peaks and ensure accurate selection, retention time, integration, and the uniformity of the peak shape for the endogenous and internal standard peptide signals.[32] For each peptide, the relative peak area ratio of the endogenous to the heavy labeled internal standard peptide was calculated. This ratio and the known concentration of internal standard peptide were used to calculate the concentration of the endogenous peptide in the sample by comparison to a standard curve generated in the pooled sample. The criteria used for the standard curve regression analysis were 1/x2 regression weighting, <15% deviation in a given level's precision and accuracy for each concentration level, and 20% at the lower limit of quantification.

DIA Data Processing. EncyclopeDIA[31] was used to generate the library and perform protein identification and quantification. The human proteome in FASTA format was obtained from UniProtKB,[33] and a spectral library containing only human proteins (pan human) was obtained from the National Institute of Standards and Technology—NIST (https://chemdata.nist.gov/dokuwiki/doku.php?id=peptidew:cdownload). These were used with the six gas phase fraction files from the analysis of the chromatogram library sample to create a human plasma-specific chromatogram library. The library was used for the identification and quantitation of the proteins in samples, with trypsin as the enzyme, CID/HCD as the fragmentation method, and 10 ppm mass tolerances for the precursor, fragment, and library mass tolerances. Percolator[34] (3.10) was used to validate the identifications with the false discovery rate set to 1%.

The MS proteomic data have been deposited to the ProteomeXchange Consortium via the PRIDE partner repository with the data set identifier PXD029437.

STATISTICAL ANALYSES

An unsupervised cluster analysis was performed on the determined protein concentrations. We used complete distance to perform the clustering on the scaled and centered concentration values. The visualization of the data using heat maps was performed after centering and scaling of the determined protein concentrations. Differences between groups were tested using the Wilcoxon rank-sum test. *P*-values were adjusted using the Benjamini−Hochberg method to account for multiple testing. The volcano plots of COVID-19 patients with healthy controls as the reference, and within the COVID-19 patient cohort for comparing survivors versus nonsurvivors, ventilated versus not ventilated, males versus females, and ARBs and ACEi exposed versus not exposed were completed based on the *p*-values of the Mann−Whitney−Wilcoxon test and calculated fold changes based on the determined protein concentration. Fold changes were calculated on a base-2 logarithmic scale after dividing the individual protein concentrations by the corresponding reference abundance of the protein, which was dictated by the comparison performed. For the baseline comparison of COVID-19 patients with the healthy controls, the reference was the mean protein abundance in the healthy controls, while for the longitudinal comparisons it was the corresponding patient protein abundance at the baseline. For the other comparisons within the COVID-19 patient group, that is, survivors versus nonsurvivors, ventilated versus not ventilated

https://doi.org/10.1021/acs.jproteome.1c00863
J. Proteome Res. 2022, 21, 975−992

(invasive ventilation), males versus females, and ARBs and ACEi exposed versus not exposed, the references were survivors, not ventilated, males, ARBs and ACEi not exposed COVID-19 patients, respectively, at all the time points. Partitional time series clustering with the Manhattan distance was used to identify protein profile clusters over time. Significantly differentiated proteins and proteins belonging to identified time series clusters were used for functional analysis which was performed using Cytoscape[35] and related plugins[36] to understand the pathways that were significantly perturbed in acute COVID-19. Data analysis and visualization were performed using R,[37] Cytoscape, and GeneMANIA Cytoscape plugin and web application.[35,36]

RESULTS

Targeted Proteomics and DIA

We determined protein concentrations in the blood plasma of acute COVID-19 patients and externally acquired controls using two approaches, MRM and DIA. Targeted protein quantification with internal standards is suited for longitudinal and multicentric studies because it references measured intensity to spiked-in internal standards. It has been previously demonstrated that plasma proteomics can identify up to 900 proteins.[38] Quantification, however, also relies on additional criteria, namely that protein-determined concentrations in samples are within the dynamic range of a standard curve that is generated as part of the experiment. Here, we used a quantitative proteomic panel for 270 plasma proteins, which we were able to quantify in human plasma in various previous experiments.[28,30,39] The panel included internal standards for all the targeted proteins (Table S1) and has been characterized previously as showing good reproducibility.[30] In a parallel experiment, we measured all the samples using the discovery DIA method.[40,41] The results from the DIA method were used mainly for validation purposes and comparison with MRM results. The quantification based on MRM was used for the comparison between groups.

In our absolute quantitative MRM proteomics, we were able to detect 196 proteins, of which 171 were quantified. We considered a protein not quantifiable if its concentration in all the samples was below the limit of quantification (LLOQ), which was determined from the standard curve that was generated in the same experiment.[26] All quantified proteins were used in the further evaluation of the differences between groups (Table S1). No imputation was performed, and we used a nonparametric test for our comparisons.

Using the DIA method, we were able to identify 203 protein groups. 56% of all the DIA-identified proteins were covered by three or less peptides, while apolipoprotein B-100 (APOB) with 126 peptides was the protein with the largest coverage in terms of unique peptides. Figure S1 shows a histogram of the number of detected DIA peptides per protein. In total there were 128 detected proteins shared between the DIA and MRM methods (Figure S2). Thirty-six out of 70 proteins with no MRM assay in our panel that were detected using DIA were immunoglobulins, and another five were keratins (Table S4). Four proteins with targeted assays in our panel that were not detectable using MRM, but were identified using DIA, included coagulation factor X (F10), E-selectin (SELE), melanotransferrin (MELTF), and phosphatidylcholine-sterol acyltransferase (LCAT). All four were identified using DIA with a single peptide, and only the LCAT peptide matched the surrogate peptide in the failed MRM assay (SSGLVSNAPGVQIR). When examining this peptide closely in our MRM data, it turned out that it had a valid standard curve and intensity with an acquired signal above LLOQ, but it had interference in all the measured samples and controls and therefore was not considered as quantifiable, examples are shown in Figure S3. Figure S4, on the other hand, shows an example of the increasing intensity over time of the peptide TYLPAVDEK surrogate for apolipoprotein C-II (APOC2) in one acute COVID-19 patient. This protein appeared in one of the longitudinal clusters that we will discuss below in the section regarding the longitudinal analysis.

Excellent correlations between the results of the two methods we used, DIA and MRM, across all the samples were obtained (Figure S5). Because of this very good agreement between the two methods, and because of the absolute quantitative aspect of the MRM data, we focused our further analysis on the results from the absolute quantification. We performed multiple comparisons that included investigating the signature of acute COVID-19 versus healthy individuals, male versus female, exposure to ARBs, use of ACEi, use of ventilation, and the difference between survivors and nonsurvivors. Furthermore, we performed a longitudinal analysis in which we referenced patient protein levels at 2, 4, 7, and 14 days to their own baseline levels at admission. With the exception of comparing patients with healthy individuals, all our comparisons relied only on the acute COVID-19 patient samples.

COVID-19 Patients and Associated Plasma Protein Signature

The baseline characteristics of the COVID-19 patients are shown in Table 1. Patients were of mean age 65 years, 72% were males and 52% had comorbidities, most commonly hypertension (43%). ARBs and ACEi were used prior to admission in 7 and 11%, respectively. The treatment in hospitals included mechanical ventilation (35%), vasopressors (34%), and renal replacement therapy (10%). The hospital mortality was 22%, with a mean time to death of 23 days. Controls (n = 30) consisted of 24 male and six female healthy blood donors with a mean age of 37.3 years and their baseline characteristics are listed in Table 1.

Figure 1 shows a volcano plot comparison of protein levels in acute COVID-19 patients at baseline versus healthy controls. Of all the proteins quantified, 29 were significantly higher in abundance in acute COVID-19 patients than healthy controls (Benjamini−Hochberg corrected p-value < 0.05 and at least twofold higher) and two proteins that were significantly lower (Benjamini−Hochberg corrected p-value < 0.05 and at least twofold lower). The proteins with higher abundance included: actin-aortic smooth muscle (ACTA2), α-1-acid glycoprotein 1 (ORM1), α-1-antichymotrypsin (SERPINA3), β-2-microglobulin (B2M), carbonic anhydrase 1 (CA1), complement component C9 (C9), C-reactive protein (CRP), cystatin-c (CST3), follistatin-related protein 1 (FSTL1), fructose−bisphosphate aldolase b (ALDOB), haptoglobin (HP), hemoglobin subunit α (HBA1; HBA2), insulin-like growth factor-binding protein 2 (IGFBP2), leucine-rich α-2-glycoprotein (LRG1), lipopolysaccharide-binding protein (LBP), matrix metalloproteinase-9 (MMP9), neutrophil gelatinase-associated lipocalin (LCN2), osteopontin (SPP1), peroxiredoxin-2 (PRDX2), plasma protease c1 inhibitor (SERPING1), pregnancy zone protein (PZP), protein s100-

https://doi.org/10.1021/acs.jproteome.1c00863
J. Proteome Res. 2022, 21, 975−992

Table 1. Baseline Characteristics of COVID-19 Patients and Healthy Controls, Including Mortality, Use of Invasive Ventilation, and Use of ARBs and ACEi in Patients with COVID-19[a]

	COVID-19 patients									
		28-day mortality		Invasive mechanical ventilation		Sex		ARBs/ACEi[b]		
Variable	COVID-19 (n=46)	No (n=38)	Yes (n=8)	No (n=30)	Yes (n=16)	Male (n=33)	Female (n=13)	No ARBs/ACEi (n=34)	ARBs (n=4)	ACEi (n=8)
Age										
Median (IQR)	64.5 (52.0, 79.0)	58.5 (49.0, 72.0)	87.0 (79.0, 91.5)	68.5 (48.0, 81.0)	63.0 (58.0, 73.5)	63.0 (55.0, 79.0)	68.0 (42.0, 80.0)	58.5 (48.0, 76.0)	66.5 (59.0, 70.5)	79.5 (75.0, 84.0)
Range	(34.0, 94.0)	(34.0, 90.0)	(66.0, 94.0)	(34.0, 94.0)	(48.0, 90.0)	(40.0, 94.0)	(34.0, 90.0)	(34.0, 94.0)	(55.0, 71.0)	(55.0, 90.0)
Sex, n (%)										
Male	33 (71.7)	27 (71.1)	6 (75.0)	19 (63.3)	14 (87.5)	33 (100.0)	0 (0.0)	25 (73.5)	3 (75.0)	5 (62.5)
Female	13 (28.3)	11 (28.9)	2 (25.0)	11 (36.7)	2 (12.5)	0 (0.0)	13 (100.0)	9 (26.5)	1 (25.0)	3 (37.5)
Co-morbidities, n (%) ^										
Any of the following	24 (52.2)	18 (47.4)	6 (75.0)	17 (56.7)	7 (43.8)	18 (54.5)	6 (46.2)	12 (35.3)	4 (100.0)	8 (100.0)
Chronic cardiac disease	10 (21.7)	7 (18.4)	3 (37.5)	9 (30.0)	1 (6.3)	7 (21.2)	3 (23.1)	6 (17.6)	0 (0.0)	4 (50.0)
Chronic kidney disease	5 (10.9)	2 (5.3)	3 (37.5)	3 (10.0)	2 (12.5)	4 (12.1)	1 (7.7)	3 (8.8)	0 (0.0)	2 (25.0)
Diabetes	13 (28.3)	9 (23.7)	4 (50.0)	8 (26.7)	5 (31.3)	12 (36.4)	1 (7.7)	7 (20.6)	3 (75.0)	3 (37.5)
With complications	3 (6.5)	1 (2.6)	2 (25.0)	2 (6.7)	1 (6.3)	3 (9.1)	0 (0.0)	3 (8.8)	0 (0.0)	0 (0.0)
Without complications	10 (21.7)	8 (21.1)	2 (25.0)	6 (20.0)	4 (25.0)	9 (27.3)	1 (7.7)	4 (11.8)	3 (75.0)	3 (37.5)
Hypertension	20 (43.5)	14 (36.8)	6 (75.0)	13 (43.3)	7 (43.8)	15 (45.5)	5 (38.5)	8 (23.5)	4 (100.0)	8 (100.0)
ARBs prior to admission, n (%)	4 (8.7)	4 (10.5)	0 (0.0)	1 (3.3)	3 (18.8)	3 (9.1)	1 (7.7)	0 (0.0)	4 (100.0)	0 (0.0)
ACE inhibitors prior to admission, n (%)	8 (17.4)	6 (15.8)	2 (25.0)	7 (23.3)	1 (6.3)	5 (15.2)	3 (23.1)	0 (0.0)	0 (0.0)	8 (100.0)
Admitted to ICU, n (%)	20 (43.5)	15 (39.5)	5 (62.5)	4 (13.3)	16 (100.0)	16 (48.5)	4 (30.8)	15 (44.1)	3 (75.0)	2 (25.0)
Treatment during hospitalization										
ARBs, n (%)	3/44 (6.8)	3/36 (8.3)	0/8 (0.0)	2/29 (6.9)	1/15 (6.7)	2/33 (6.1)	1/11 (9.1)	1/33 (3.0)	2/4 (50.0)	0/7 (0.0)
ACEi, n (%)	5/45 (11.1)	4/37 (10.8)	1/8 (12.5)	5/30 (16.7)	0/15 (0.0)	2/33 (6.1)	3/12 (25.0)	1/33 (3.0)	0/4 (0.0)	4/8 (50.0)
Mechanical ventilation, n (%)	16/46 (34.8)	12/38 (31.6)	4/8 (50.0)	0/30 (0.0)	16/16 (100.0)	14/33 (42.4)	2/13 (15.4)	12/34 (35.3)	3/4 (75.0)	1/8 (12.5)
RRT, n (%)	4/41 (9.8)	2/34 (5.9)	2/7 (28.6)	0/29 (0.0)	4/12 (33.3)	4/29 (13.8)	0/12 (0.0)	3/29 (10.3)	1/4 (25.0)	0/8 (0.0)
Vasopressors, n (%)	15/45 (33.3)	10/37 (27.0)	5/8 (62.5)	2/30 (6.7)	13/15 (86.7)	13/33 (39.4)	2/12 (16.7)	13/33 (39.4)	1/4 (25.0)	1/8 (12.5)
Antiviral agent, n (%)	8/45 (17.8)	6/37 (16.2)	2/8 (25.0)	4/30 (13.3)	4/15 (26.7)	6/33 (18.2)	2/12 (16.7)	7/33 (21.2)	0/4 (0.0)	1/8 (12.5)
Patient in-hospital outcome, n (%)										
Still in hospital	1 (2.2)	1 (2.6)	0 (0.0)	0 (0.0)	1 (6.3)	0 (0.0)	1 (7.7)	1 (2.9)	0 (0.0)	0 (0.0)
Death	10 (21.7)	3 (7.9)	7 (87.5)	3 (10.0)	7 (43.8)	9 (27.3)	1 (7.7)	9 (26.5)	0 (0.0)	1 (12.5)
Discharged alive	28 (60.9)	27 (71.1)	1 (12.5)	24 (80.0)	4 (25.0)	17 (51.5)	11 (84.6)	20 (58.8)	2 (50.0)	6 (75.0)
Discharged to other facility	7 (15.2)	7 (18.4)	0 (0.0)	3 (10.0)	4 (25.0)	7 (21.2)	0 (0.0)	4 (11.8)	2 (50.0)	1 (12.5)
Hospital length of stay (among those who discharged alive) (days)										
Median (IQR)	7.0 (3.5, 14.0)	7.0 (3.0, 14.0)	8.0 (8.0, 8.0)	7.0 (3.0, 10.5)	17.5 (13.0, 28.5)	7.0 (3.0, 11.0)	8.0 (4.0, 17.0)	7.0 (3.0, 14.0)	21.5 (4.0, 39.0)	7.5 (7.0, 11.0)
Mean (SD)	10.5 (10.8)	10.6 (11.0)	8.0 (.)	8.8 (9.7)	20.8 (12.8)	9.5 (9.2)	12.0 (13.4)	8.5 (6.0)	21.5 (24.7)	13.5 (17.3)
Range	(0.0, 48.0)	(0.0, 48.0)	(8.0, 8.0)	(0.0, 48.0)	(9.0, 39.0)	(0.0, 39.0)	(0.0, 48.0)	(0.0, 19.0)	(4.0, 39.0)	(0.0, 48.0)
Discharged from ICU, n (%)										
Still in ICU	1 (5.0)	1 (6.7)	0 (0.0)	0 (0.0)	1 (6.3)	0 (0.0)	1 (25.0)	1 (6.7)	0 (0.0)	0 (0.0)
Death in ICU	6 (30.0)	2 (13.3)	4 (80.0)	1 (25.0)	5 (31.3)	6 (37.5)	0 (0.0)	5 (33.3)	0 (0.0)	1 (50.0)
Discharged alive from ICU	13 (65.0)	12 (80.0)	1 (20.0)	3 (75.0)	10 (62.5)	10 (62.5)	3 (75.0)	9 (60.0)	3 (100.0)	1 (50.0)
ICU length of stay (among those who discharged from ICU alive) (days)										
Median (IQR)	9.5 (5.5, 23.0)	10.0 (5.0, 29.0)	9.0 (9.0, 9.0)	3.0 (1.0, 8.0)	12.0 (9.0, 29.0)	12.0 (6.0, 29.0)	8.0 (1.0, 9.0)	8.5 (5.5, 13.5)	29.0 (12.0, 43.0)	3.0 (3.0, 3.0)
Mean (SD)	14.6 (13.2)	15.1 (13.7)	9.0 (.)	4.0 (3.6)	18.1 (13.4)	17.4 (14.0)	6.0 (4.4)	11.0 (9.7)	28.0 (15.5)	3.0 (.)
Range	(1.0, 43.0)	(1.0, 43.0)	(9.0, 9.0)	(1.0, 8.0)	(5.0, 43.0)	(3.0, 43.0)	(1.0, 9.0)	(1.0, 32.0)	(12.0, 43.0)	(3.0, 3.0)
Time to death (among those who died) (days)										
Median (IQR)	17.0 (13.0, 36.0)	37.0 (36.0, 62.0)	13.0 (4.0, 20.0)	4.0 (3.0, 14.0)	24.0 (13.0, 37.0)	20.0 (13.0, 36.0)	13.0 (13.0, 13.0)	20.0 (13.0, 36.0)	-	13.0 (13.0, 13.0)
Mean (SD)	22.6 (18.1)	45.0 (14.7)	13.0 (7.7)	7.0 (6.1)	29.3 (17.4)	23.7 (18.8)	13.0 (.)	23.7 (18.8)	-	13.0 (.)
Range	(3.0, 62.0)	(36.0, 62.0)	(3.0, 24.0)	(3.0, 14.0)	(13.0, 62.0)	(3.0, 62.0)	(13.0, 13.0)	(3.0, 62.0)	-	(13.0, 13.0)

	Healthy controls	
	Sex	
Variable	Male (n=24)	Female (n=6)
Age		
Median (IQR)	35 (28.75, 41)	46.5 (40,48.5)
Range	(18, 57)	(19,50)
Race		
Black	62.50%	0%
Hispanic	33%	100%
Caucasian	4.10%	0%

[a]Multiple categories can be selected for each patient. [b]Abbreviations: ARB, angiotensin receptor blocker; ACEi, angiotensin-converting enzyme inhibitor; ICU, intensive care unit; and RRT, renal replacement therapy.

A12 (S100A12), protein s100-A9 (S100A9), protein deglycase dj-1/parkinson disease protein 7 (PARK7), serum amyloid A-1 and A-2 proteins (SAA1; SAA2), serum amyloid P-component (APCS), secreted protein acidic and rich in cysteine (SPARC), thrombospondin-1 (THBS1), vascular cell adhesion protein 1 (VCAM1, vascular cell adhesion molecule 1), and von Willebrand factor (VWF). The two proteins with significantly decreased abundance were cartilage acidic protein 1 (CRTAC1) and serum paroxynase/lactonase 3 (PON3). Table S2 lists the proteins with their functions as available from UniProtKB and associated Gene Ontology terms.

A heat map of the COVID-19 patients versus healthy controls illustrates the marked differences in plasma protein levels between COVID-19 patients (admission levels only) and healthy controls (Figure 2). The hierarchical clustering guiding the orders in Figure 2 discriminated almost perfectly between healthy controls and COVID-19 patients. The horizontal clustering on the protein axis divided the map into multiple sections of proteins with increased or decreased abundance, which can also be seen in the volcano plot (Figure 1). The protein associations with specific functions are shown such as various complement component proteins in the second cluster.

Table 2 and Figure 3 list and show the results of an interaction/pathway analysis of the proteins with significantly increased ($p < 0.05$) abundances that showed at least a twofold increase compared to healthy controls. Pathway ontology classes included acute inflammatory response, complement activation, regulation of inflammatory response, and regulation of protein activation cascade.

Longitudinal Trends in Plasma Protein Levels of COVID-19 Patients

The time course analysis of protein levels in the COVID-19 patients showed distinct protein profiles (Figure S6 and Table S3). We identified the following specific profiles of proteins over time: increasing, rapid decrease followed by recovery, sudden decrease followed by an increase, and steady levels maintained over time (Figure 4). The analysis of these profiles revealed increased levels of lipid associated functions. The complement activation, humoral immune response, and general protein activation cascade were associated with proteins showing a rapid decrease followed by recovery. Proteins associated with acute inflammatory response also showed a rapid decrease followed by a slower increase, but to a lesser extent than complement related proteins. Finally, the rapid decrease followed by an increase was observed in proteins associated with the regulation of smooth muscle cell proliferation and migration and secretory mechanisms and platelet degranulation.

Additional Identified Patterns

The three proteins S100A-9, S100-A12, and apolipoprotein(a) (LPA) showed a significant difference between survivors and nonsurvivors (Figure 5). For this analysis all the data points were considered.

Four proteins that differed between ARB inhibitor users and non-users including increased complement factor B (CFB), ALDOB, IgGFc−binding protein (FCGBP), and decreased VCAM1. There were also two proteins differentiated in their abundance between ACEi users and non-users; ALDOB and S100-A9 both showed decreased abundance in the users of ACE (Figure 6).

https://doi.org/10.1021/acs.jproteome.1c00863
J. Proteome Res. 2022, 21, 975−992

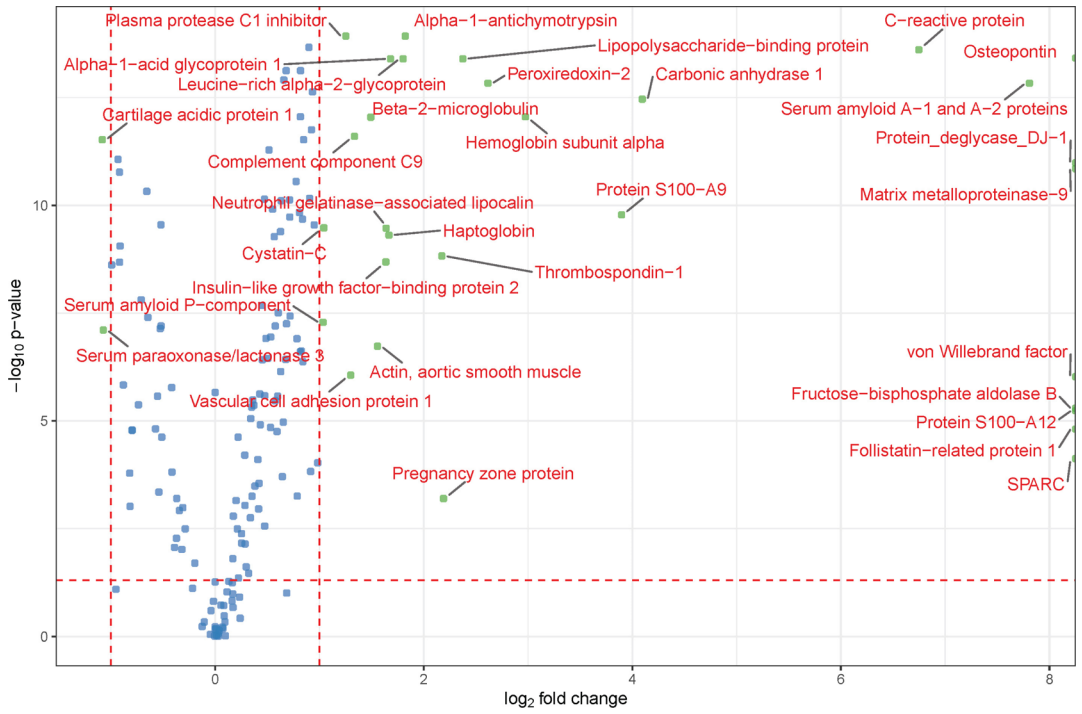

Figure 1. Comparison of protein levels in COVID-19 patients and healthy controls. The volcano plot indicating fold change (x-axis) and negative $\log_{10}$ p-value (y-axis) for each protein comparison of patients who had COVID-19 with controls. The vertical dashed line indicates boundaries of $\log_2$ fold change (lower or higher) and the vertical dashed line indicates $p < 0.05$. p-values were adjusted for multiple testing using the Benjamini−Hochberg method.

Only PZP was significantly different in abundance according to sex using the threshold that we applied, that is, adjusted p-value < 0.05 and a twofold change in protein abundance.

No difference in the level of the measured proteins was determined between ventilated patients versus not ventilated.

DISCUSSION

Plasmas Protein Signature of COVID-19

In our analysis, 29 proteins were overexpressed, and two proteins were underexpressed in COVID-19 patients compared to healthy controls. Several proteins with higher abundance are known as acute-phase reactants (CRP, LBP, and B2M) and have been previously reported to be increased in COVID-19 patients. These acute-phase reactants reflect distinct pathways: CRP is a marker of IL-6 activation (or IL-1−IL-6), while B2M is a marker of lymphocyte turnover. Additionally, three amyloid proteins, of which two are acute-phase reactants SAA1 and SAA2, showed increased abundance in patients. While using complement inhibition is under investigation as therapy in COVID-19,[42] there were few differentiating proteins in our analysis that were associated with the complement cascade. Other pathway associations might provide novel targets for biomarkers and/or as drug targets (Figure 3). Several differentially expressed proteins are known to be localized to erythrocytes, which makes them undetectable in plasma unless there is significant hemolysis or possible sample contamination. These included HBA1, HBA2, PARK7, PRDX2, HB, ALDOB, and CA1. We investigated whether this was a result of poor sample preparation that led to erythrocyte contamination of the plasma, and compared the differentially abundant proteins with the erythrocyte and platelet contaminants identified by Geyer et al.[38] Only two out of the 31 differentially abundant proteins are known to be possible erythrocyte contaminants, that is, CA1 and PRDX2, and only one is known to be a possible platelet contaminant, that is, THBS1. Although these results await independent validation, they might imply an increased hemolysis in COVID-19 patients, which raises questions about whether erythrocytes are more susceptible to hemolysis in COVID-19 patients and whether there is a causal correlation between the hemolysis level and disease severity. Along with future independent validation, these questions may be a focus for further research on COVID-19 severity.

The difference in mean age between the COVID-19 patients and healthy controls was 28 years. To investigate possible effects of the age difference, we compared all the 31 discriminating proteins to the 72 plasma proteins known to be correlated and predictors of age as described by Tanaka et al.[43] In their work, Tanaka et al. used aptamer-based SOMAscan assays to measure the relative abundance of 1301 proteins. Only one single protein of the 72 age predictors was in the set of discriminating proteins between healthy controls and COVID-19 patients, that is, IGFBP2. In order to further be more specific in our comparison, we calculated using the data from Tanaka et al. a projected increase in abundance of 1.57 (β = 0.018) over 25 years for the top age-predicting protein, that is, growth differentiation factor 15 (GDF15). Top age-predicting protein corresponds to the largest absolute slope (β) value, which means all other age related increase or decrease in protein abundance would correspond to a lower fold change. To that end, all the discriminating proteins between healthy and acute COVID-19 patients that we reported on had a minimum fold change of two, which is much larger than 1.57.

Comparisons within the patient groups, that is, without using control samples included effects of sex, ARB exposure,

https://doi.org/10.1021/acs.jproteome.1c00863
J. Proteome Res. 2022, 21, 975−992

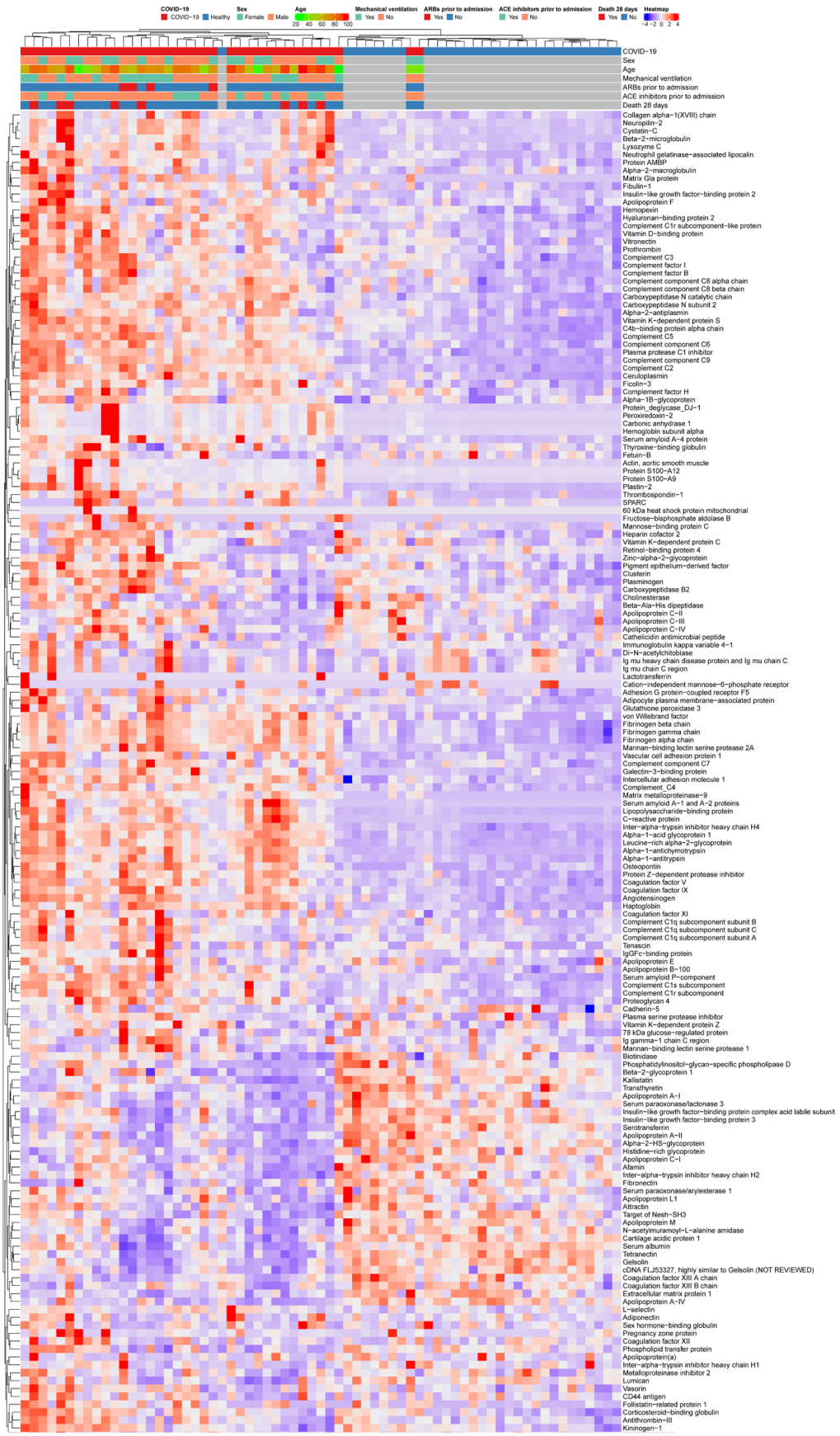

Figure 2. Heat map of protein levels in COVID-19 patients and healthy controls. The horizontal blue line at the top indicates controls and the horizontal red line at the top indicates COVID-19 patients. The heat map colors range from blue for decreased levels to red for increased levels, with shades indicating the relative size of change. Individual subjects are in columns and individual proteins are in rows.

https://doi.org/10.1021/acs.jproteome.1c00863
J. Proteome Res. 2022, 21, 975−992

Table 2. Enriched Protein Functions when Comparing COVID-19 Patients with Healthy Controls and in the Identified Protein Longitudinal Time Profiles

	Proteins	Enriched GO Term
COVID-19 vs. healthy control (Figure 3)	CRTAC1 , MMP9 , CST3 , PON3 , VWF , SPARC , C9 , IGFBP2 , PARK7 , SPP1 , PZP , LBP , CRP , APCS , CA1 , SAA2 , ALDOB , THBS1 , LCN2 , SERPING1 , VCAM1 , S100A9 , S100A12 , FSTL1 , B2M , PRDX2 , LRG1 , SAA1 , HBA2 , SERPINA3 , ORM1 , HP	inflammatory response acute inflammatory response protein activation cascade complement activation regulation of inflammatory response regulation of protein activation cascade
Time series group 1 (Figure 4A)	HSPA5, APOC2, CAMP, F13A1, COL18A1, FN1, EEA1, ALDOB, HP, SERPIND1, IGHG1, IGHM, IGHM, ICAM1, LUM, LYZ, MBL2, CST3, PLTP, SERPINA5, ABI3BP, CLEC3B, THBS1, VASN, PEPD	vesicle lumen cytoplasmic membrane-bounded vesicle lumen heparin binding plasma lipoprotein particle protein-lipid complex glycosaminoglycan binding sulfur compound binding
Time series group 2 (Figure 4B)	ACTC1, A1BG, SERPINC1, ATRN, CNDP1, CP, F5, C1QB, C1QC, C1R, C1RL, C5, C8B, CFI, ECM1, FGA, FGB, FGG, FBLN1, GSN, HPX, ITIH4, MASP1, MASP2, TIMP2, PGLYRP2, SERPING1, SHBG, TNC, VCAM1, PROS1, PROZ	protein activation cascade complement activation blood microparticle humoral immune response regulation of protein activation cascade regulation of complement activation regulation of humoral immune response
Time series group 8 (Figure 4C)	ADIPOQ, A2M, APOD, APOL1, LPA, B2M, CDH5, NA, BCHE, CFH, IGFBP3, IGFALS, AMBP, SPARC	secretory granule lumen regulation of smooth muscle cell proliferation smooth muscle cell proliferation vesicle lumen cytoplasmic membrane-bounded vesicle lumen platelet degranulation regulation of smooth muscle cell migration
Time series group 9 (Figure 4D)	SERPINA1, SERPINF2, APOC4, APOE, APOF, CRTAC1, CLU, C1S, C3, C7, SERPINA6, CTBS, FETUB, HABP2, PLG, PZP, S100A12, SERPINA10, F2, TF, ALB, PON1, PON3, SERPINA7, GC	regulation of protein processing high-density lipoprotein particle enzyme inhibitor activity plasma lipoprotein particle protein activation cascade protein-lipid complex endopeptidase inhibitor activity

and use of ACEi. There was little difference in the signature of the measured proteins between males and females in the COVID-19 patients with only one protein, PZP. PZP is an α2 globulin that increases during pregnancy, modulates the immune function and is also associated with Alzheimer's disease[44] and inflammatory conditions.

A few proteins were overexpressed in ARB-exposed versus non-ARB-exposed COVID-19 patients, including CFB, ALDOB, and FCGBP, while one protein showed decreased abundance, VCAM1. ARBs alter the proteomic response in other conditions such as myocardial ischemia models[45,46] and thus, ARBs could alter the plasma proteomes of acute COVID-19 patients. Interestingly, FCGBP was also one of the two proteins that showed a significant decrease in abundance in the users of ACEi, together with S100-A9.

Notably, only S100A-9, S100-A12, and LPA were different between survivors and nonsurvivors. S100A9 has been associated with increased mortality in COVID-19.[47,48] S100A9 interacts with S100A8 to modulate vascular inflammation and lymphocyte recruitment to the sites of infection and is central to sepsis responses[49] and is associated with increased sepsis mortality.[50]

The functional analysis of the differentiated proteins in COVID-19 patients compared to healthy controls resulted in the enrichment of multiple annotations pointing to an activated immune and inflammation response (Table 2, Figure 3). This is in agreement with previous reports on COVID-19 immunopathogenesis.[51] The ontology classes included acute inflammatory response, complement activation, regulation of inflammatory response, and regulation of protein activation cascade. Each of these pathways is important in the acute, immune, and complex protein responses to infection by SARS-CoV-2. This is in agreement with previous reports. Shen and colleagues[19] found activation of three major pathways: the complement system, macrophage function, and platelet degranulation.

Longitudinal Analysis

Analyzing the plasma protein abundances of hospitalized acute COVID-19 patients revealed several distinct patterns that included resolution (sustained decrease), decrease followed by increase, or greater disruption over the 14 day observation period.

One protein group of the time series clusters identified in COVID-19 patients (Figure 4B, Table 2, Figure S6, and Table S2) was associated with the immune response, similar to the results we obtained when comparing acute COVID-19 patients versus healthy controls. In a profile showing rapid decrease in concentrations followed by recovered plasma levels, the proteins in this group, were associated with activation and regulation of the complement and humoral systems. Proteins associated with acute inflammatory response also showed a similar trend in cluster 4 (Figure S6).

Clusters 1 and 9 (Figure 4A, D), which represented two opposing trends, that is, an increase for proteins in cluster 1 and decrease for those in cluster 9, were both associated with the protein−lipid complex. However, while the profile related to increased abundance over time was associated with multiple

https://doi.org/10.1021/acs.jproteome.1c00863
J. Proteome Res. 2022, 21, 975−992

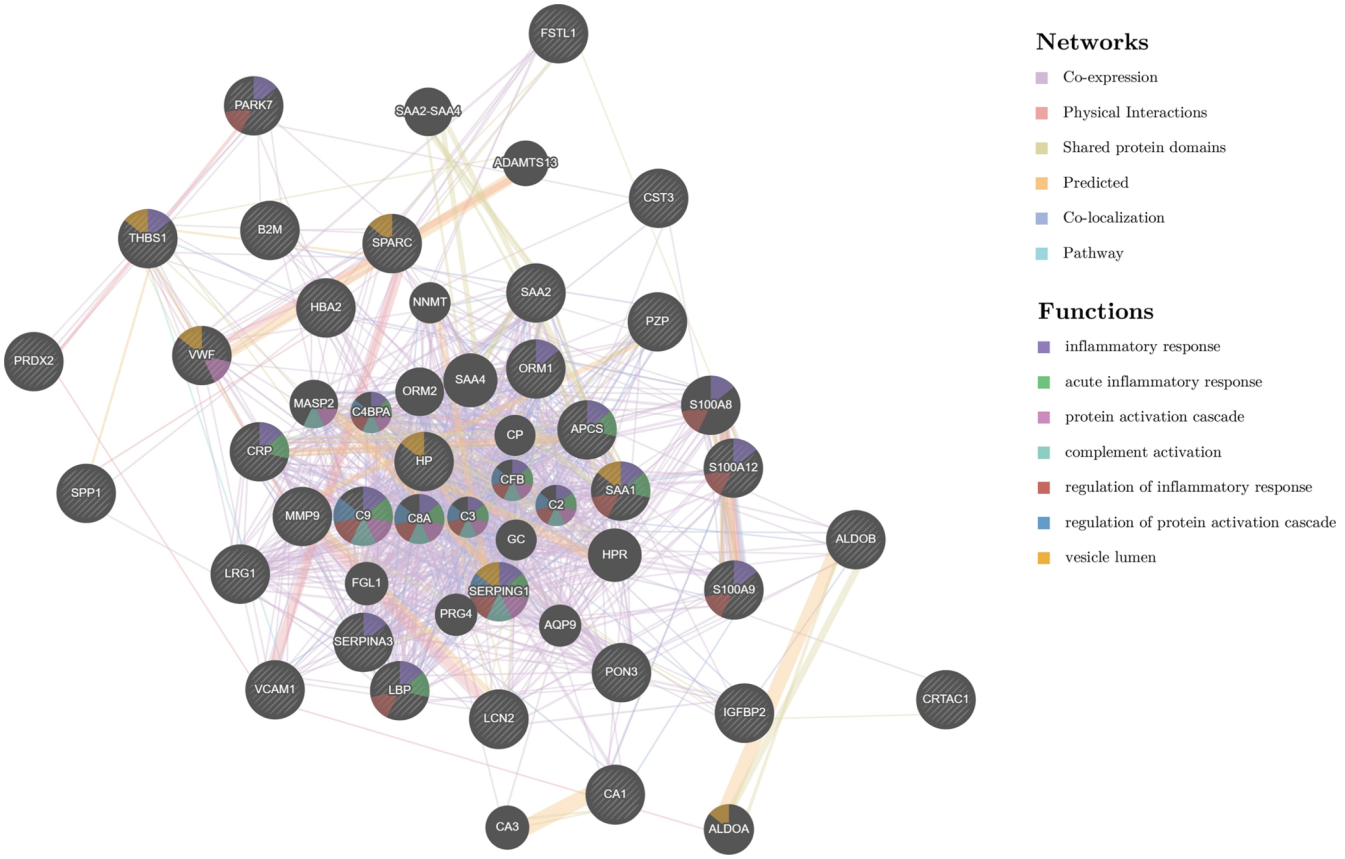

Figure 3. Pathways interactions of the significantly increased (p-value < 0.05 and at least twofold increase COVID-19 compared to healthy controls. p-values were adjusted for multiple testing using the Benjamini−Hochberg method).

binding activities including heparin, glycosaminoglycan, and sulfur compound binding, the opposing profile was associated with enzyme inhibiting activities related to multiple serine protease inhibitors. This outlines a continuous decrease in these functions (over the first 14 days), which might explain findings in a recent study that identified altered lipid metabolism when studying red blood cells in COVID-19 patients compared to healthy.[52] The relation between SERPIN family proteins and COVID-19, including some in the current study, was also discussed in recent works.[53−56] Our results showed a distinct longitudinal profile that indicates a delayed response and decrease in abundance of the measured SERPINs.

One interesting trend that grouped multiple proteins that exhibited a rapid decrease followed by an increase in abundance, cluster 8 (Figure 4, Figure S6). These proteins were related to platelet degranulation, secretory mechanisms, and the regulation of smooth muscle cell proliferation.

Interpretation and Potential Clinical Aspects

To our knowledge, this is the first report of proteomic analysis investigating patients with acute COVID-19 over the first 14 days of hospitalization. Shen and colleagues[19] found that 93 plasma proteins were differentially regulated in COVID-19 patients at the baseline compared to controls, showing the dysregulation of pathways that modulate macrophages, platelets, the complement system, and metabolic suppression. Park and colleagues[57] identified 76 proteins (indicating alterations of neutrophil activation, complement activation, platelet function, T cell suppression and pro-inflammatory factors upstream and downstream of interleukin-6, interleukin-1B, and tumor necrosis factor) that differed between moderate and severe COVID-19. Shu and colleagues[58] also discovered significant alterations of immune or inflammatory responses, platelet degranulation, coagulation, and metabolism.

Increased acute-phase reactants such as CRP and LBP (a marker of intestinal leakage) increased in patients with COVID-19 who have cardiac injury,[59] B2M (increased in the cerebrospinal fluid of COVID-19[60]) and ORM1 (previously reported in COVID-19[61]) indicate the brisk host response to SARS-CoV-2 infection in hospitalized patients. Although it is true that these are all acute-phase reactants, they reflect distinct pathways: CRP is a marker of IL-6 activation (or IL-1 activating IL-6), while B2M is a marker of lymphocyte turnover.

Three amyloid-related proteins were increased in COVID-19 compared to healthy controls and these are acute-phase proteins, which was also observed by Shen and colleagues.[19] Although await validation, these could be indicators of cognitive dysfunction and depression after COVID-19 because of their association with Alzheimer's disease and depression. SAA1 and SAA2 were increased in our COVID-19 patients, and are known to be increased in sepsis,[62,63] Alzheimer's disease, and depression.[64] The survivors of COVID-19 have increased risks of cognitive difficulties and depression[65] suggesting that increased serum amyloid A1 and/or A2 could be candidate biomarkers of these neurological complications of COVID-19. APCS (the serum form of amyloid P, a component of amyloid plaques in brain), which was also increased in our COVID-19 patients, is a biomarker of

https://doi.org/10.1021/acs.jproteome.1c00863
J. Proteome Res. 2022, 21, 975−992

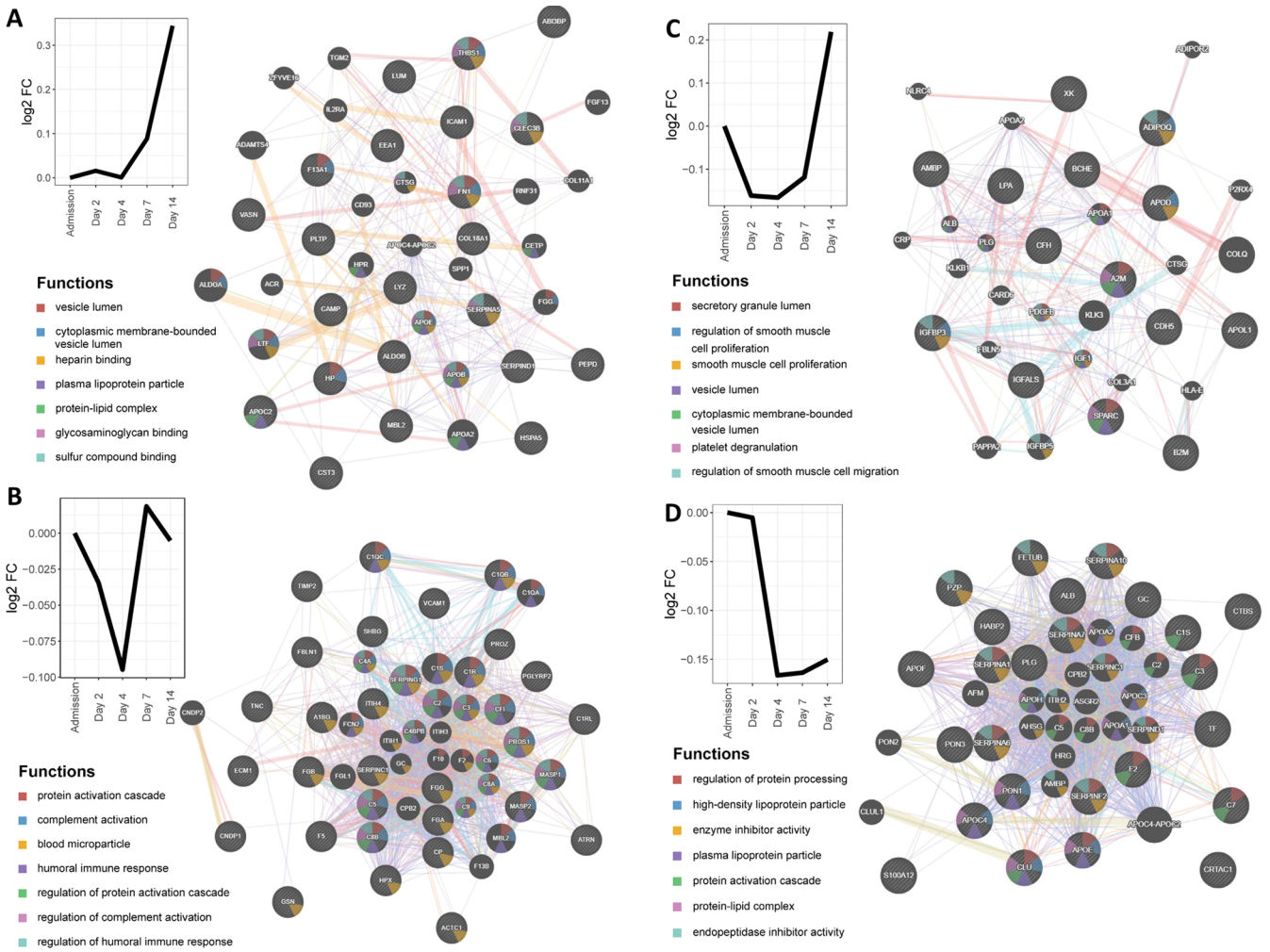

Figure 4. Time course of protein levels in the COVID-19 patients. Of nine measured longitudinal protein concentration profiles that were identified using time series cluster analysis, four groups were selected based on the clear distinct profile. The functional analysis of the protein members of these groups, using known interactions and gene ontology annotations, resulted in the specific functions reported in the figure.

Alzheimer's disease[66,67] and a drug target for amyloid disorders.[68,69]

We also found that SPARC abundance was elevated in the COVID-19 patient plasma and it is another protein known to be associated with depression (e.g., bipolar depression,[70] modulates brain function in Alzheimer's disease[71] and depression[72]) and is overexpressed in peripheral blood monocytes in acute respiratory distress syndrome.[73]

Protein s100-A12 was increased in COVID-19 patient plasma and is a widely studied protein, an alarmin, pro-inflammatory protein that is increased in conditions such as diabetes,[74] stent thrombosis, and sepsis-induced acute respiratory distress syndrome, and predicts an increased risk of death in sepsis.[50] Protein s100-A9 was also increased, but to our knowledge, not previously reported in COVID-19 patients previously. The increase of protein s100-A9 in the plasma in various cancers (e.g., chronic lymphocytic leukemia,[75] hepatocellular cancer,[76] diabetic complications,[77] and pulmonary tuberculosis[78]) has been thoroughly reviewed previously.

Other proteins increased in COVID-19 patients compared to healthy controls in our study, but not reported in prior studies on COVID-19 patients included SERPINA3, FSTL1, ALDOB, HB, HBA1/HBA2, IGFBP2, LRG1, LCN2 (reported in urine[79] but not in plasma from COVID-19 patients), PRDX2, SERPING1, PZP, PARK7, SPARC, and THBS1. Several of these proteins point to increased hemolysis in COVID-19 patients.

Enhanced coagulation is an important part of the pathophysiology of severe COVID-19 and we found increased levels of THBS1 in our COVID-19 patients that had not been reported previously in COVID-19; THBS1 is a pro-inflammatory matrix glycoprotein that modulates endothelial cell adhesion, platelet adhesion, and interacts with a host of adhesion factors and proteases. THBS1 is a marker of disseminated intravascular coagulation in sepsis[80] and this may be relevant in COVID-19 because of the frequent and often complicated course (e.g., deep venous thrombosis and pulmonary emboli) of increased coagulation in COVID-19.[81−83]

Other proteins that we found were increased in COVID-19 have been reported by others. Our finding of increased CA1 aligns with observations that carbonic anhydrases interact with the renin-angiotensin system in the pathogenesis of SARS-CoV-2 in the respiratory, renal, and cardiovascular systems.[84] CST3 was higher in COVID-19 patients than in healthy controls and has been reported previously as a marker of more severe COVID-19.[85−87] MMP-9 was also increased in COVID-19 patients as reported previously[88] and in acute respiratory

https://doi.org/10.1021/acs.jproteome.1c00863
J. Proteome Res. 2022, 21, 975−992

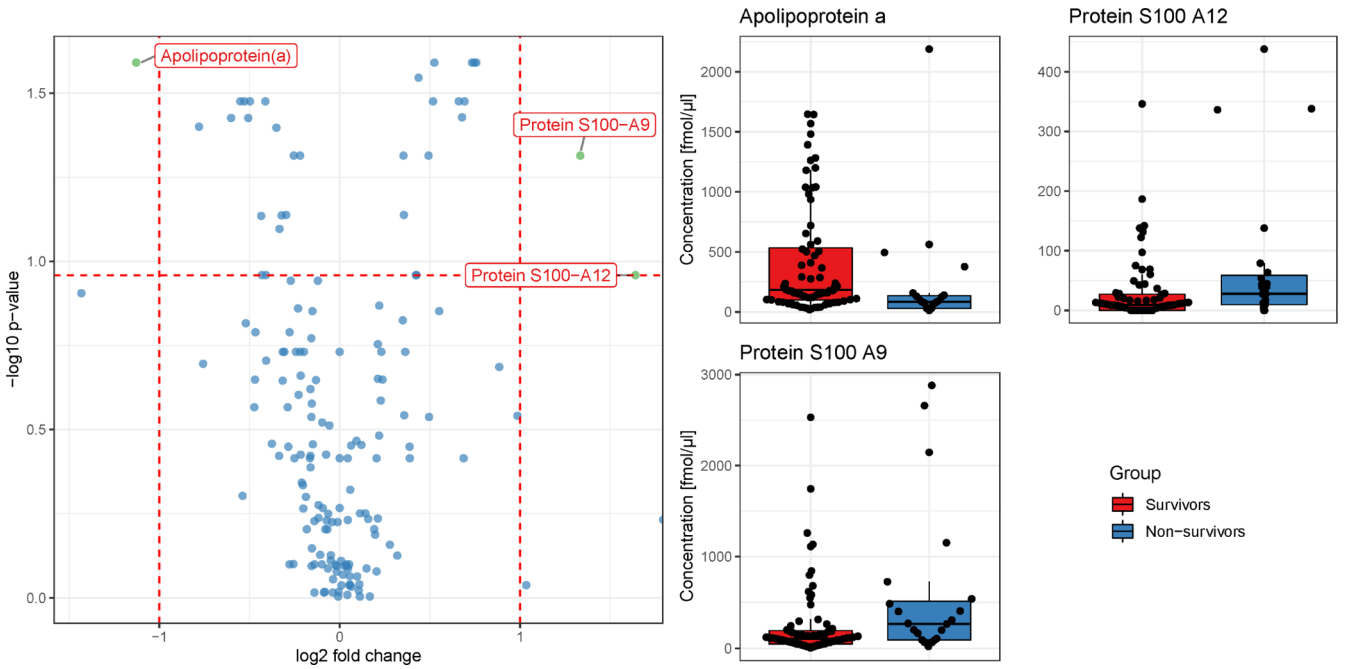

Figure 5. Proteins that differed between COVID-19 survivors and nonsurvivors. The volcano plot indicating fold change (x-axis) and negative $\log_{10}$ p-value (y axis) for each protein comparison of survivors and nonsurvivors of the COVID-19 patients. The vertical dashed line indicates boundaries of $\log_2$ fold change (lower of higher) and the vertical dashed line indicates $p < 0.05$. p-values were adjusted for multiple testing using the Benjamini−Hochberg method.

distress syndrome not due to COVID-19.[89] SPP1was increased in our study and was higher in severe compared to nonsevere COVID-19 in another study.[90] SPP1 is a cytokine-like matrix-associated phosphoglycoprotein that increases furin expression.[91] Furin is a proprotein convertase that activates precursors of chemokines, growth factors, hormones, adhesion molecules, and receptors and promotes SARS-CoV-2 cell entry and replication. We and others[92] showed that VCAM 1 was increased in COVID-19 patients. VCAM1 is also increased in sepsis,[93] it is a marker of bacteremia in sepsis[94] and correlates with an increased risk of multiple organ failure in sepsis.[95] VWF was increased in our COVID-19 cases and has been published before in COVID-19 in general[96] and as a marker of coagulopathy,[97] venous thrombosis,[98] and of acute kidney injury in COVID-19.[99]

Strengths and Limitations of Current Work

The strengths of our study include the relatively large sample size of acute COVID-19 hospitalized patients in whom we had repeated measurements over 14 days of plasma protein levels, the multicenter design enhancing generalizability, healthy controls for comparison, the assessment of multiple protein levels to understand the proteomic response in early acute COVID-19, and the evaluation of the association of ARBs and ACEi use with protein levels in plasma.

The possible limitations of our study were that we included samples that were collected at hospital admission and over 14 subsequent days of hospitalization such that we cannot infer what effects COVID-19 has on plasma protein levels at earlier, pre-hospital or later times (in- and post-hospital). The number of patients with exposure to ARBs and ACEi is small, and therefore our associated results regarding proteins with different plasma levels require further validation. Another possible limitation is that the control group had relatively few Caucasians and that they were likely healthy (because they were blood donors) but we do not know if they had any comorbidities. Finally, the fact that blood was processed within a 4 h window from collection in the laboratories may be a limitation.

We performed multiple comparisons using only the samples from acute COVID-19 patients, this included investigating proteomic signature of sex, of exposure to ARBs, of ACEi, of ventilation, and the difference between survivors and non-survivors. Furthermore, in our longitudinal analysis we made use of only patient samples and referenced each to own baseline protein levels. In one analyses, namely comparing acute COVID-19 with healthy individuals, we used external set of plasma samples. Although this is not ideal and we cannot control for differences in sample preparation procedures and were not able to perform age matching, we followed three points to assert the validity of this comparison. First, the COVID-19 samples were collected in a multicentric effort and, therefore, these samples themselves comprise differences in sample preparation. Hence, differences in sample preparation are, to some degree, accounted for implicitly. Second, there were no significant differences that pointed out any known contamination from sample preparation, as we highlighted earlier. Third, all the discriminating proteins were included at a fold change threshold of two. This threshold is higher than the maximum reported protein abundance difference in healthy humans, with a 25 year difference as we mentioned earlier. Thus, while the two sample sets may seem not ideal for comparison, our investigation and relating our results to previous works, on plasma contamination due to sample preparation and the effect of age, merit the comparison. Nonetheless, our findings require validation in subsequent acute COVID-19 cohorts in order to be able to generalize the results. Future studies should also evaluate plasma protein levels early in the course of COVID to determine when in the pre-hospital course changes in plasma protein levels occur.

https://doi.org/10.1021/acs.jproteome.1c00863
J. Proteome Res. 2022, 21, 975−992

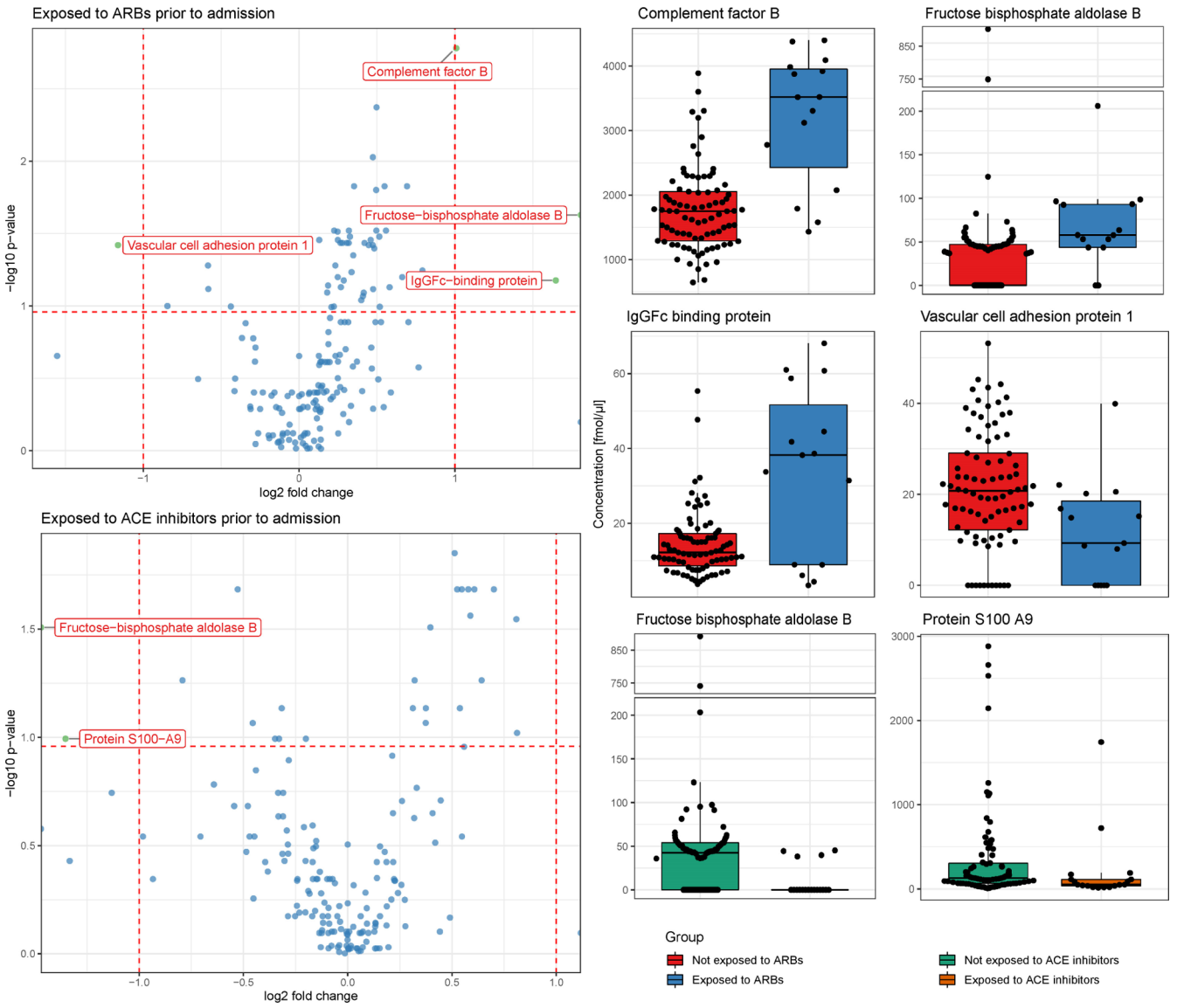

Figure 6. Protein levels according to ARBs or ACEi exposure prior to hospital admission for acute COVID-19. The volcano plots show protein fold change (x-axis) and negative $\log_{10}$ p-value (y axis) for each protein comparison of patients who had COVID-19 and were or were not on ARBs/ACE prior to hospital admission for acute COVID-19. The vertical dashed line indicates boundaries of $\log_2$ fold change (lower of higher) and the vertical dashed line indicates $p < 0.05$. Boxplots show the differentially abundant proteins. p-values were adjusted for multiple testing using the Benjamini−Hochberg method.

Additional studies may evaluate the association of changes in proteomics in acute COVID-19 patients with "COVID-19 long haul" syndromes in survivors, and we still need to understand whether and when changes in proteomics in acute COVID-19 patients return to normal in post-hospital discharge patients.

CONCLUSIONS

Several expected (e.g., CRP and LBP) and many unexpected proteins differed in their plasma levels between COVID-19 patients and healthy controls that indicated activated pathways that had differing recovery trajectories over 14 days. These novel proteins and pathways may be targets for the biomarkers of COVID-19 and/or possible therapeutic targets. We showed for the first time, several amyloid-related proteins that are increased in Alzheimer's disease and depression were also increased in acute COVID-19, and we speculated that they could be biomarkers of cognitive dysfunction and depression in survivors of COVID-19. Finally, the different patterns of proteome network disruption versus resolution over the 14 day observation period may help guide the timing of interventions because the treatment of COVID-19 requires attention to the clinical and likely the proteomic phases (e.g., viral, inflammatory, and hypercoagulable) of COVID-19.

ASSOCIATED CONTENT

Supporting Information

The Supporting Information is available free of charge at https://pubs.acs.org/doi/10.1021/acs.jproteome.1c00863.

Histogram of protein coverage in DIA; overlap in detected proteins between MRM and DIA methods; interference in the endogenous signal of LCAT surrogate peptide SSGLVSNAPGVQIR; increasing endogenous signal of APOC2 in one acute COVID-19 patient over time as shown by its surrogate peptide

https://doi.org/10.1021/acs.jproteome.1c00863
J. Proteome Res. 2022, 21, 975−992

TYLPAVDEK; correlations between targeted proteomics and DIA methods; identified protein abundance trends over time; targeted proteomic panel with protein detectability and quantifiability; discriminating proteins between COVID-19 patients and healthy controls; longitudinal time series clustering and protein members of each group; and identified proteins using MRM and DIA (PDF)

AUTHOR INFORMATION

Corresponding Authors

Yassene Mohammed − *Genome BC Proteomics Centre, University of Victoria, Victoria V8Z 5N3 British Columbia, Canada; Center for Proteomics and Metabolomics, Leiden University Medical Center, Leiden 2333 ZA, Netherlands;* orcid.org/0000-0003-3265-3332; Phone: +31 715266878; Email: y.mohammed@lumc.nl

James A. Russell − *Centre for Heart Lung Innovation and Division of Critical Care Medicine, St. Paul's Hospital, University of British Columbia, Vancouver V6Z 1Y6 British Columbia, Canada*; Phone: (604) 806-8346; Email: Jim.Russell@hli.ubc.ca

Authors

David R. Goodlett − *Genome BC Proteomics Centre, University of Victoria, Victoria V8Z 5N3 British Columbia, Canada; Department of Biochemistry and Microbiology, University of Victoria, Victoria V8W 2Y2 British Columbia, Canada; International Centre for Cancer Vaccine Science, University of Gdansk, Gdansk 80-822, Poland*

Matthew P. Cheng − *Division of Infectious Diseases (Department of Medicine), Division of Medical Microbiology (Department of Pathology and Laboratory Medicine), McGill University Health Centre, Montreal H4A 3J1 Quebec, Canada*

Donald C. Vinh − *Division of Infectious Diseases (Department of Medicine), Division of Medical Microbiology (Department of Pathology and Laboratory Medicine), McGill University Health Centre, Montreal H4A 3J1 Quebec, Canada*

Todd C. Lee − *Department of Medicine, McGill University, Montreal H4A 3J1 Quebec, Canada*

Allison Mcgeer − *Mt. Sinai Hospital and University of Toronto, Toronto M5G 1X5 Ontario, Canada*

David Sweet − *Division of Critical Care Medicine, Department of Emergency Medicine, Vancouver General Hospital and University of British Columbia, Vancouver V5Z 1M9 British Columbia, Canada*

Karen Tran − *Division of General Internal Medicine, Vancouver General Hospital and University of British Columbia, Vancouver V5Z 1M9 British Columbia, Canada*

Terry Lee − *Centre for Health Evaluation and Outcome Science (CHEOS), St. Paul's Hospital, University of British Columbia, Vancouver V6Z 1Y6 British Columbia, Canada*

Srinivas Murthy − *BC Children's Hospital, University of British Columbia, Vancouver V6H 3N1 British Columbia, Canada*

John H. Boyd − *Centre for Heart Lung Innovation and Division of Critical Care Medicine, St. Paul's Hospital, University of British Columbia, Vancouver V6Z 1Y6 British Columbia, Canada*

Joel Singer − *Centre for Health Evaluation and Outcome Science (CHEOS), St. Paul's Hospital, University of British Columbia, Vancouver V6Z 1Y6 British Columbia, Canada*

Keith R. Walley − *Centre for Heart Lung Innovation and Division of Critical Care Medicine, St. Paul's Hospital, University of British Columbia, Vancouver V6Z 1Y6 British Columbia, Canada*

David M. Patrick − *British Columbia Centre for Disease Control (BCCDC) and University of British Columbia, Vancouver V5Z 4R4 British Columbia, Canada*

Curtis Quan − *Department of Medicine, McGill University, Montreal H4A 3J1 Quebec, Canada*

Sara Ismail − *Department of Medicine, McGill University, Montreal H4A 3J1 Quebec, Canada*

Laetitia Amar − *Department of Medicine, McGill University, Montreal H4A 3J1 Quebec, Canada*

Aditya Pal − *Department of Medicine, McGill University, Montreal H4A 3J1 Quebec, Canada*

Rayhaan Bassawon − *Department of Medicine, McGill University, Montreal H4A 3J1 Quebec, Canada*

Lara Fesdekjian − *Department of Medicine, McGill University, Montreal H4A 3J1 Quebec, Canada*

Karine Gou − *Department of Medicine, McGill University, Montreal H4A 3J1 Quebec, Canada*

Francois Lamontagne − *University of Sherbrooke, Sherbrooke J1K 2R1 Quebec, Canada*

John Marshall − *Department of Surgery, St. Michael's Hospital, Toronto M5B 1W8 Ontario, Canada*

Greg Haljan − *Division of Critical Care, Surrey Memorial Hospital and University of British Columbia, Surrey V3V 1Z2 British Columbia, Canada*

Robert Fowler − *Sunnybrook Health Sciences Centre, Toronto M4N 3M5 Ontario, Canada*

Brent W. Winston − *Departments of Critical Care Medicine, Medicine and Biochemistry and Molecular Biology, University of Calgary, Calgary T2N 4N1 Alberta, Canada*

ARBs CORONA I

Complete contact information is available at: https://pubs.acs.org/10.1021/acs.jproteome.1c00863

Author Contributions

Conception and design: J.A.R. and D.R.G. Analysis: Y.M. Interpretation: Y.M., D.R.G., M.P.C., D.C.V., T.C.L., A.M., D.S., K.T., T.L., S.M., J.H.B., J.S., K.R.W., D.M.P., C.Q., S.I., L.A., A.P., R.B., L.F., K.G., F.L., J.M., G.H., R.F., B.W.W., and J.A.R. Drafting the manuscript for important intellectual content: Y.M., D.R.G., M.P.C., D.C.V., T.C.L., A.M., D.S., K.T., T.L., S.M., J.H.B., J.S., K.R.W., D.M.P., C.Q., S.I., L.A., A.P., R.B., L.F., K.G., F.L., J.M., G.H., R.F., B.W.W., and J.A.R.

Notes

The authors declare the following competing financial interest(s): Dr. Russell reports patents owned by the University of British Columbia (UBC) that are related to the use of PCSK9 inhibitor(s) in sepsis and related to the use of vasopressin in septic shock and a patent owned by Ferring for use of selepressin in septic shock. Dr. Russell is an inventor on these patents. Dr. Russell was a founder, Director, and shareholder in Cyon Therapeutics, Inc. and is a shareholder in Molecular You Corp. Dr. Russell reports receiving consulting fees in the last 3 years from: 1. Asahi Kesai Pharmaceuticals of America (AKPA) (was developing recombinant thrombomodulin in sepsis). 2. SIB Therapeutics

https://doi.org/10.1021/acs.jproteome.1c00863
J. Proteome Res. 2022, 21, 975−992

LLC (developing a sepsis drug). 3. Ferring Pharmaceuticals (manufactures vasopressin and developing selepressin). Dr. Russell is no longer actively consulting for the following: La Jolla Pharmaceuticals (developing angiotensin II; Dr. Russell chaired the DSMB of a trial of angiotensin II from 2015 to 2017) and PAR Pharma (sells prepared bags of vasopressin). Dr. Russell reports having received an investigator-initiated grant from Grifols (titled "Is HBP a mechanism of albumins efficacy in human septic shock?") that was provided to and administered by UBC. Matthew P. Cheng and Donald C. Vinh have a patent application pending (Electronic Filing System ID: 40101099). Donald C. Vinh has a report of invention submitted to McGill University (Track code D2021-0043). Donald C. Vinh is supported by the Fonds de la recherche en sant du Qubec clinician-scientist scholar Junior 2 program. He has received clinical trial support from Cidara Therapeutics, CSL Behring, and Janssen Pharmaceuticals as well as consulting or speaker honoraria from CSL Behring, Merck Canada, Novartis Canada, and UCB Biosciences GmbH. All other authors state that they have no competing interests.

■ ACKNOWLEDGMENTS

We thank the patients and families who participated in the ARBs CORONA I study, which has increased our understanding of COVID-19. We also thank the many dedicated clinicians (doctors, nurses, therapists, and others) who cared for these patients and comforted their families. This study was supported in part by a grant from the Canadian Institutes of Health Research [grant # 442999: Host Response Mediators in Coronavirus (2019-nCoV) Infection—Is There a Protective Effect of Angiotensin II Type 1 Blockers on Outcomes of Coronavirus Infection?] to J.A.R., St. Paul's Hospital Foundation to J.A.R., and for Drs. Goodlett and Mohammed by the Genome Canada and Genome British Columbia grants (204PRO, 214PRO, 264PRO, and 282PQP) and the International Centre for Cancer Vaccine Science project, which is carried out within the International Research Agendas program of the Foundation for Polish Science co-financed by the European Union under the European Regional Development Fund (MAB/2017/03). We are thankful for the ARBs CORONA I support from the Canadian Institutes of Health Research, grant number: 439993 and St. Paul's Hospital Foundation to J.A.R. John Boyd is a recipient of a Providence Health Care Research Scholarship. Keith Walley is supported by Canadian Institutes of Health Research (CIHR) Foundation Grant FDN 154311. We thank Dr. Azad Eshghi for his valuable comments that led to improving the results we presented in this work. **ARBs CORONA I Study Consortium Role**. The ARBs CORONA I Consortium consists of leading researchers at St. Paul's Hospital, Centre for Health Evaluation and Outcomes Science, University of Victoria Genome BC Proteomics Centre, British Columbia Women's and Children's Hospital, Vancouver General Hospital, Royal Columbian Hospital, Surrey Memorial Hospital, British Columbia Centres for Disease Control, University of British Columbia, CHUS, McGill University Health Centre, Sunnybrook Hospital, Toronto University Health Network, Mount Sinai Hospital in Toronto, Kingston General Hospital, University of Ottawa, Winnipeg Health Sciences Centre, Foothills Hospital, University of Alberta, University of Pennsylvania, Peking Medical College, and Phramongkutklao Army Hospital. Dr. Russell is principal investigator of the grant to support this study. The consortium members at St. Paul's Hospital and CHEOS wrote the grants, coordinated the study, got ethics approval, designed the Case Report Forms and the database, did the statistical analyses, and wrote first draft. The University of Victoria Genome BC Proteomics Centre performed the proteomics analyses and the related aspects of the statistical and enrichment analyses. The clinical sites contributed patient identification and obtained plasma and clinical information in the Case Report Form. Other members listed below contributed to the grants to support this work and to the interpretation of results and the writing of the manuscript. *British Columbia*: St. Paul's Hospital, Vancouver, BC, Canada: Drs. James Russell, Nadia Khan, John Boyd, Keith Walley, Anita Palepu, Adeera Levin. Centre for Health Evaluation and Outcomes Science (CHEOS), St. Paul's Hospital, Vancouver, BC, Canada: Drs. Joel Singer, Terry Lee. British Columbia Women's and Children's Hospital, Vancouver, BC, Canada: Dr. Srinivas Murthy. Vancouver General Hospital, Vancouver, BC, Canada: Drs. Nathaniel Hawkins, Shane Arishenkoff, David Sweet. Royal Columbian Hospital, New Westminster, BC, Canada: Dr Steve Reynolds. Surrey Memorial Hospital, Surrey, BC, Canada: Dr. Greg Haljan. British Columbia Centres for Disease Control: Dr. David Patrick. Xenon Pharmaceutical and University of British Columbia, Vancouver, BC, Canada: Dr. Simon Pimstone. *Province of Quebec*: CHUS, Sherbrooke, PQ, Canada: Dr. Francois Lamontagne. McGill University Health Centre, Montreal, PQ, Canada: Dr. Matthew P. Cheng, Dr. Todd C. Lee, Dr. Lucie Roussel (Vinh lab), Dr. Donald C. Vinh. *Ontario*: Sunnybrook Hospital, Toronto, Ont., Canada: Dr. Robert Fowler. University Health Network, Toronto, Ont., Canada: Dr. John Granton. Mount Sinai Hospital, Toronto, Ont., Canada: Dr. Allison McGeer. St Michael's Hospital, Toronto, Ont., Canada: Drs. John Marshall, Art Slutsky. Kingston General Hospital, Kingston, Ont., Canada: Drs. David Maslove, Santiago Perez Patrigeon. University of Ottawa, Ottawa, Ont., Canada: Dr. Kevin Burns. *Manitoba*: Winnipeg Health Sciences Centre, Winnipeg, Man., Canada: Dr. Anand Kumar. *Alberta*: Foothills Hospital, Calgary, Alberta, Canada: Dr. Brent Winston. University of Alberta, Edmonton, Alberta, Canada: Dr. Oleksa Rewa. *USA*: University of Pennsylvania, Philadelphia, PA, USA: Dr. Michael Harhay. *China*: Peking Medical College, Beijing, China: Dr. Du Bin. *Thailand*: Phramongkutklao Army Hospital, Bangkok. The following persons and institutions participated in the ARBs CORONA I Study: *Steering Committee*: J. A. Russell (chair), Genevieve Rocheleau (former project manager), Puneet Mann (project manager), D. Sweet, G. Haljan, M. Cheng, D. Vinh, T. Lee, F. Lamontagne, B. Winston, O. Rewa, J. Marshall, A. McGeer, R. Fowler, David Maslove, Santiago Perez Patrigeon. *Management Committee*: J. A. Russell (chair), Genevieve Rocheleau (project manager), Puneet Mann (project manager), Karen Tran, Joel Singer. *Data Management*: J. Singer, T. Lee. **ARBs CORONA I Investigators and Centers**. *Canada*. *British Columbia*: St. Paul's Hospital (Coordinating Centre): J. A. Russell, K. R. Walley, J. Boyd, T. Lee, J. Singer. Vancouver General Hospital: D. Sweet, K. Tran. Royal Columbian Hospital: S. Reynolds. Surrey Memorial Hospital: G. Haljan. University of Victoria Genome BC Proteomics Laboratory: Y. Mohammed, D. Goodlett. *Quebec*: McGill University Centre Hospital: M. Cheng, D. Vinh. Jewish General Hospital: T. Lee. Sherbrooke: F. Lamontagne. *Alberta*: Calgary General Hospital: B. Winston. University of Alberta: O. Rewa. *Ontario*: St. Michael's Hospital: J. Marshall, A. Slutsky. Mount Sinai Hospital: A.

https://doi.org/10.1021/acs.jproteome.1c00863
J. Proteome Res. 2022, 21, 975−992

McGeer, V. Sivanantham. Sunnybrook and Women's College Health Science Centre: R. Fowler. Kingston General Hospital: David Maslove, Santiago Perez Patrigeon.

REFERENCES

(1) Bohn, M. K.; Hall, A.; Sepiashvili, L.; Jung, B.; Steele, S.; Adeli, K. Pathophysiology of COVID-19: Mechanisms Underlying Disease Severity and Progression. *Physiology* **2020**, *35*, 288−301.
(2) Hanna, R.; Dalvi, S.; Sălăgean, T.; Pop, I. D.; Bordea, I. R.; Benedicenti, S. Understanding COVID-19 Pandemic: Molecular Mechanisms and Potential Therapeutic Strategies. An Evidence-Based Review. *J. Inflamm. Res.* **2021**, *14*, 13−56.
(3) Harrison, A. G.; Lin, T.; Wang, P. Mechanisms of SARS-CoV-2 Transmission and Pathogenesis. *Trends Immunol.* **2020**, *41*, 1100−1115.
(4) Sokolowska, M.; Lukasik, Z. M.; Agache, I.; Akdis, C. A.; Akdis, D.; Akdis, M.; Barcik, W.; Brough, H. A.; Eiwegger, T.; Eljaszewicz, A.; Eyerich, S.; Feleszko, W.; Gomez-Casado, C.; Hoffmann-Sommergruber, K.; Janda, J.; Jiménez-Saiz, R.; Jutel, M.; Knol, E. F.; Kortekaas Krohn, I.; Kothari, A.; Makowska, J.; Moniuszko, M.; Morita, H.; O'Mahony, L.; Nadeau, K.; Ozdemir, C.; Pali-Schöll, I.; Palomares, O.; Papaleo, F.; Prunicki, M.; Schmidt-Weber, C. B.; Sediva, A.; Schwarze, J.; Shamji, M. H.; Tramper-Stranders, G. A.; Veen, W.; Untersmayr, E. Immunology of COVID-19: Mechanisms, clinical outcome, diagnostics, and perspectives-A report of the European Academy of Allergy and Clinical Immunology (EAACI). *Allergy* **2020**, *75*, 2445−2476.
(5) Gordon, D. E.; Jang, G. M.; Bouhaddou, M.; Xu, J.; Obernier, K.; O'Meara, M. J.; Guo, J. Z.; Swaney, D. L.; Tummino, T. A.; Huttenhain, R.; Kaake, R. M.; Richards, A. L.; Tutuncuoglu, B.; Foussard, H.; Batra, J.; Haas, K.; Modak, M.; Kim, M.; Haas, P.; Polacco, B. J.; Braberg, H.; Fabius, J. M.; Eckhardt, M.; Soucheray, M.; Bennett, M. J.; Cakir, M.; McGregor, M. J.; LiNaing, Q. Z. Z. C.; Zhou, Y.; Peng, S.; Kirby, I. T.; Melnyk, J. E.; Chorba, J. S.; Lou, K.; Dai, S. A.; Shen, W.; Shi, Y.; Zhang, Z.; Barrio-Hernandez, I.; Memon, D.; Hernandez-ArmentaMathy, C. C. J. P.; Perica, T.; Pilla, K. B.; Ganesan, S. J.; Saltzberg, D. J.; Ramachandran, R.; Liu, X.; Rosenthal, S. B.; Calviello, L.; Venkataramanan, S.; LinWankowicz, Y. S. A.; Bohn, M.; Trenker, R.; Young, J. M.; Cavero, D.; Hiatt, J.; Roth, T.; Rathore, U.; Subramanian, A.; Noack, J.; Hubert, M.; Roesch, F.; ValletMeyer, T. B.; White, K. M.; Miorin, L.; Agard, D.; Emerman, M.; Ruggero, D.; Garcia-Sastre, A.; Jura, N.; von Zastrow, M.; Taunton, J.; Schwartz, O.; Vignuzzi, M.; d'EnfertMukherjee, C. S.; Jacobson, M.; Malik, H. S.; Fujimori, D. G.; Ideker, T.; Craik, C. S.; Floor, S.; Fraser, J. S.; Gross, J.; Sali, A.; Kortemme, T.; Beltrao, P.; Shokat, K.; Shoichet, B. K.; Krogan, N. J. A SARS-CoV-2-Human Protein-Protein Interaction Map Reveals Drug Targets and Potential Drug-Repurposing. *Nature* **2020**, *583* (7816), 459−468.
(6) Shang, J.; Ye, G.; Shi, K.; Wan, Y.; Luo, C.; Aihara, H.; Geng, Q.; Auerbach, A.; Li, F. Structural basis of receptor recognition by SARS-CoV-2. *Nature* **2020**, *581*, 221−224.
(7) Ou, X.; Liu, Y.; Lei, X.; Li, P.; Mi, D.; Ren, L.; Guo, L.; Guo, R.; Chen, T.; Hu, J.; Xiang, Z.; Mu, Z.; Chen, X.; Chen, J.; Hu, K.; Jin, Q.; Wang, J.; Qian, Z. Characterization of spike glycoprotein of SARS-CoV-2 on virus entry and its immune cross-reactivity with SARS-CoV. *Nat. Commun.* **2020**, *11*, 1620.
(8) Letko, M.; Marzi, A.; Munster, V. Functional assessment of cell entry and receptor usage for SARS-CoV-2 and other lineage B betacoronaviruses. *Nat. Microbiol.* **2020**, *5*, 562−569.
(9) Zhou, P.; Yang, X.-L.; Wang, X.-G.; Hu, B.; Zhang, L.; Zhang, W.; Si, H.-R.; Zhu, Y.; Li, B.; Huang, C.-L.; Chen, H.-D.; Chen, J.; Luo, Y.; Guo, H.; Jiang, R.-D.; Liu, M.-Q.; Chen, Y.; Shen, X.-R.; Wang, X.; Zheng, X.-S.; Zhao, K.; Chen, Q.-J.; Deng, F.; Liu, L.-L.; Yan, B.; Zhan, F.-X.; Wang, Y.-Y.; Xiao, G.-F.; Shi, Z.-L. A pneumonia outbreak associated with a new coronavirus of probable bat origin. *Nature* **2020**, *579*, 270−273.
(10) Xu, X.; Chen, P.; Wang, J.; Feng, J.; Zhou, H.; Li, X.; Zhong, W.; Hao, P. Evolution of the novel coronavirus from the ongoing Wuhan outbreak and modeling of its spike protein for risk of human transmission. *Sci. China Life Sci.* **2020**, *63*, 457−460.
(11) Li, M.-Y.; Li, L.; Zhang, Y.; Wang, X.-S. Expression of the SARS-CoV-2 cell receptor gene ACE2 in a wide variety of human tissues. *Infect. Dis. Poverty* **2020**, *9*, 45.
(12) Macedo, A.; Gonçalves, N.; Febra, C. COVID-19 fatality rates in hospitalized patients: systematic review and meta-analysis. *Ann. Epidemiol.* **2021**, *57*, 14−21.
(13) Bojkova, D.; Klann, K.; Koch, B.; Widera, M.; Krause, D.; Ciesek, S.; Cinatl, J.; Münch, C. Proteomics of SARS-CoV-2-infected host cells reveals therapy targets. *Nature* **2020**, *583*, 469−472.
(14) Gordon, D. E.; Jang, G. M.; Bouhaddou, M.; Xu, J.; Obernier, K.; White, K. M.; O'Meara, M. J.; Rezelj, V. V.; Guo, J. Z.; Swaney, D. L.; Tummino, T. A.; Hüttenhain, R.; Kaake, R. M.; Richards, A. L.; Tutuncuoglu, B.; Batra, H.; Batra, J.; Haas, K.; Modak, M.; Kim, M.; Haas, P.; Polacco, B. J.; Braberg, H.; Fabius, J. M.; Eckhardt, M.; Soucheray, M.; Bennett, M. J.; Cakir, M.; McGregor, M. J.; Li, Q.; Meyer, B.; Roesch, F.; Vallet, T.; Mac Kain, A.; Miorin, L.; Moreno, E.; Naing, Z. Z. C.; Zhou, Y.; Peng, S.; Shi, Y.; Zhang, Z.; Shen, W.; Kirby, I. T.; Melnyk, J. E.; Chorba, J. S.; Lou, K.; Dai, S. A.; Barrio-Hernandez, I.; Memon, D.; Hernandez-Armenta, C.; Lyu, J.; Mathy, C. J. P.; Perica, T.; Pilla, K. B.; Ganesan, S. J.; Saltzberg, D. J.; Rakesh, R.; Liu, X.; Rosenthal, S. B.; Calviello, L.; Venkataramanan, S.; Liboy-Lugo, J.; Lin, Y.; Huang, X.-P.; Liu, Y.; Wankowicz, S. A.; Bohn, M.; Safari, M.; Ugur, F. S.; Koh, C.; Savar, N. S.; Tran, Q. D.; Shengjuler, D.; Fletcher, S. J.; O'Neal, M. C.; Cai, Y.; Chang, J. C. J.; Broadhurst, D. J.; Klippsten, S.; Sharp, P. P.; Wenzell, N. A.; Kuzuoglu-Ozturk, D.; Wang, H.-Y.; Trenker, R.; Young, J. M.; Cavero, D. A.; Hiatt, J.; Roth, T. L.; Rathore, U.; Subramanian, A.; Noack, J.; Hubert, M.; Stroud, R. M.; Frankel, A. D.; Rosenberg, O. S.; Verba, K. A.; Agard, D. A.; Ott, M.; Emerman, M.; Jura, N.; von Zastrow, M.; Verdin, E.; Ashworth, A.; Schwartz, O.; d'Enfert, C.; Mukherjee, S.; Jacobson, M.; Malik, H. S.; Fujimori, D. G.; Ideker, T.; Craik, C. S.; Floor, S. N.; Fraser, J. S.; Gross, J. D.; Sali, A.; Roth, B. L.; Ruggero, D.; Taunton, J.; Kortemme, T.; Beltrao, P.; Vignuzzi, M.; García-Sastre, A.; Shokat, K. M.; Shoichet, B. K.; Krogan, N. J. A SARS-CoV-2 protein interaction map reveals targets for drug repurposing. *Nature* **2020**, *583*, 459−468.
(15) Geyer, P. E.; Arend, F. M.; Doll, S.; Louiset, M. L.; Virreira Winter, S.; Müller-Reif, J. B.; Torun, F. M.; Weigand, M.; Eichhorn, P.; Bruegel, M.; Strauss, M. T.; Holdt, L. M.; Mann, M.; Teupser, D. High-resolution serum proteome trajectories in COVID-19 reveal patient-specific seroconversion. *EMBO Mol. Med.* **2021**, *13*, No. e14167.
(16) Meier, F.; Beck, S.; Grassl, N.; Lubeck, M.; Park, M. A.; Raether, O.; Mann, M. Parallel Accumulation-Serial Fragmentation (PASEF): Multiplying Sequencing Speed and Sensitivity by Synchronized Scans in a Trapped Ion Mobility Device. *J. Proteome Res.* **2015**, *14*, 5378−5387.
(17) Fernandez-Lima, F. A.; Kaplan, D. A.; Park, M. A. Note: Integration of trapped ion mobility spectrometry with mass spectrometry. *Rev. Sci. Instrum.* **2011**, *82*, 126106.
(18) Mun, D.-G.; Vanderboom, P. M.; Madugundu, A. K.; Garapati, K.; Chavan, S.; Peterson, J. A.; Saraswat, M.; Pandey, A. DIA-Based Proteome Profiling of Nasopharyngeal Swabs from COVID-19 Patients. *J. Proteome Res.* **2021**, *20*, 4165−4175.
(19) Shen, B.; Yi, X.; Sun, Y.; Bi, X.; Du, J.; Zhang, C.; Quan, S.; Zhang, F.; Sun, R.; Qian, L.; Ge, W.; Liu, W.; Liang, S.; Chen, H.; Zhang, Y.; Li, J.; Xu, J.; He, Z.; Chen, B.; Wang, J.; Yan, H.; Zheng, Y.; Wang, D.; Zhu, J.; Kong, Z.; Kang, Z.; Liang, X.; Ding, X.; Ruan, G.; Xiang, N.; Cai, X.; Gao, H.; Li, L.; Li, S.; Xiao, Q.; Lu, T.; Zhu, Y.; Liu, H.; Chen, H.; Guo, T. Proteomic and Metabolomic Characterization of COVID-19 Patient Sera. *Cell* **2020**, *182*, 59−72.
(20) Whetton, A. D.; Preston, G. W.; Abubeker, S.; Geifman, N. Proteomics and Informatics for Understanding Phases and Identifying Biomarkers in COVID-19 Disease. *J. Proteome Res.* **2020**, *19*, 4219−4232.
(21) Russell, J. A.; Marshall, J. C.; Slutsky, A.; Murthy, S.; Sweet, D.; Lee, T.; Singer, J.; Patrick, D. M.; Du, B.; Peng, Z.; Cheng, M.; Burns, K. D.; Harhay, M. O. Study protocol for a multicentre, prospective

https://doi.org/10.1021/acs.jproteome.1c00863
J. Proteome Res. 2022, 21, 975−992

cohort study of the association of angiotensin II type 1 receptor blockers on outcomes of coronavirus infection. *BMJ Open* **2020**, *10*, No. e040768.
(22) Chen, N.; Zhou, M.; Dong, X.; Qu, J.; Gong, F.; Han, Y.; Qiu, Y.; Wang, J.; Liu, Y.; Wei, Y.; Xia, J.; Yu, T.; Zhang, X.; Zhang, L. Epidemiological and clinical characteristics of 99 cases of 2019 novel coronavirus pneumonia in Wuhan, China: a descriptive study. *Lancet* **2020**, *395*, 507.
(23) Huang, C.; Wang, Y.; Li, X.; Ren, L.; Zhao, J.; Hu, Y.; Zhang, L.; Fan, G.; Xu, J.; Gu, X.; Cheng, Z.; Yu, T.; Xia, J.; Wei, Y.; Wu, W.; Xie, X.; Yin, W.; Li, H.; Liu, M.; Xiao, Y.; Gao, H.; Guo, L.; Xie, J.; Wang, G.; Jiang, R.; Gao, Z.; Jin, Q.; Wang, J.; Cao, B. Clinical features of patients infected with 2019 novel coronavirus in Wuhan, China. *Lancet* **2020**, *395*, 497.
(24) Wang, D.; Hu, B.; Hu, C.; Zhu, F.; Liu, X.; Zhang, J.; Wang, B.; Xiang, H.; Cheng, Z.; Xiong, Y.; Zhao, Y.; Li, Y.; Wang, X.; Peng, Z. Clinical Characteristics of 138 Hospitalized Patients With 2019 Novel Coronavirus-Infected Pneumonia in Wuhan, China. *J. Am. Acad. Audiol.* **2020**, *323*, 1061.
(25) Bhowmick, P.; Mohammed, Y.; Borchers, C. H. MRMAssayDB: an integrated resource for validated targeted proteomics assays. *Bioinformatics* **2018**, *34*, 3566−3571.
(26) Mohammed, Y.; Pan, J.; Zhang, S.; Han, J.; Borchers, C. H. ExSTA: External Standard Addition Method for Accurate High-Throughput Quantitation in Targeted Proteomics Experiments. *Proteonomics Clin. Appl.* **2018**, *12*, 1600180.
(27) Mohammed, Y.; Bhowmick, P.; Smith, D. S.; Domanski, D.; Jackson, A. M.; Michaud, S. A.; Malchow, S.; Percy, A. J.; Chambers, A. G.; Palmer, A.; Zhang, S.; Sickmann, A.; Borchers, C. H. PeptideTracker: A knowledge base for collecting and storing information on protein concentrations in biological tissues. *Proteomics* **2017**, *17*, 1600210.
(28) Percy, A. J.; Mohammed, Y.; Yang, J.; Borchers, C. H. A standardized kit for automated quantitative assessment of candidate protein biomarkers in human plasma. *Bioanalysis* **2015**, *7*, 2991−3004.
(29) Mohammed, Y.; Domański, D.; Jackson, A. M.; Smith, D. S.; Deelder, A. M.; Palmblad, M.; Borchers, C. H. PeptidePicker: a scientific workflow with web interface for selecting appropriate peptides for targeted proteomics experiments. *J. Proteonomics* **2014**, *106*, 151−161.
(30) Gaither, C.; Popp, R.; Mohammed, Y.; Borchers, C. H. Determination of the concentration range for 267 proteins from 21 lots of commercial human plasma using highly multiplexed multiple reaction monitoring mass spectrometry. *Analyst* **2020**, *145*, 3634−3644.
(31) Searle, B. C.; Pino, L. K.; Egertson, J. D.; Ting, Y. S.; Lawrence, R. T.; MacLean, B. X.; Villén, J.; MacCoss, M. J. Chromatogram libraries improve peptide detection and quantification by data independent acquisition mass spectrometry. *Nat. Commun.* **2018**, *9*, 5128.
(32) MacLean, B.; Tomazela, D. M.; Shulman, N.; Chambers, M.; Finney, G. L.; Frewen, B.; Kern, R.; Tabb, D. L.; Liebler, D. C.; MacCoss, M. J. Skyline: an open source document editor for creating and analyzing targeted proteomics experiments. *Bioinformatics* **2010**, *26*, 966−968.
(33) The UniProt Consortium. UniProt: the universal protein knowledgebase in 2021. *Nucleic Acids Res.* **2021**, *49*, D480−D489.
(34) Käll, L.; Canterbury, J. D.; Weston, J.; Noble, W. S.; MacCoss, M. J. Semi-supervised learning for peptide identification from shotgun proteomics datasets. *Nat. Methods* **2007**, *4*, 923−925.
(35) Shannon, P.; Markiel, A.; Ozier, O.; Baliga, N. S.; Wang, J. T.; Ramage, D.; Amin, N.; Schwikowski, B.; Ideker, T. Cytoscape: a software environment for integrated models of biomolecular interaction networks. *Genome Res.* **2003**, *13*, 2498−2504.
(36) Warde-Farley, D.; Donaldson, S. L.; Comes, O.; Zuberi, K.; Badrawi, R.; Chao, P.; Franz, M.; Grouios, C.; Kazi, F.; Lopes, C. T.; Maitland, A.; Mostafavi, S.; Montojo, J.; Shao, Q.; Wright, G.; Bader, G. D.; Morris, Q. The GeneMANIA prediction server: biological network integration for gene prioritization and predicting gene function. *Nucleic Acids Res.* **2010**, *38*, W214−W220 (Web Server issue).
(37) R_Core_Team. *R: A Language and Environment for Statistical Computing*; R Foundation for Statistical Computing: Vienna, Austria, 2019. www.R-project.org.
(38) Geyer, P. E.; Voytik, E.; Treit, P. V.; Doll, S.; Kleinhempel, A.; Niu, L.; Müller, J. B.; Buchholtz, M. L.; Bader, J. M.; Teupser, D.; Holdt, L. M.; Mann, M. Plasma Proteome Profiling to detect and avoid sample-related biases in biomarker studies. *EMBO Mol. Med.* **2019**, *11*, No. e10427.
(39) Mohammed, Y.; Kootte, R. S.; Kopatz, W. F.; Borchers, C. H.; Buller, H. R.; Versteeg, H. H.; Nieuwdorp, M.; van Mens, T. E. The intestinal microbiome potentially affects thrombin generation in human subjects. *J. Thromb. Haemostasis* **2019**, *18*, 642.
(40) Venable, J. D.; Dong, M.-Q.; Wohlschlegel, J.; Dillin, A.; Yates, J. R. Automated approach for quantitative analysis of complex peptide mixtures from tandem mass spectra. *Nat. Methods* **2004**, *1*, 39−45.
(41) Gillet, L. C.; Navarro, P.; Tate, S.; Röst, H.; Selevsek, N.; Reiter, L.; Bonner, R.; Aebersold, R. Targeted data extraction of the MS/MS spectra generated by data-independent acquisition: a new concept for consistent and accurate proteome analysis. *Mol. Cell. Proteomics* **2012**, *11*, O111.
(42) Polycarpou, A.; Howard, M.; Farrar, C. A.; Greenlaw, R.; Fanelli, G.; Wallis, R.; Klavinskis, L. S.; Sacks, S. Rationale for targeting complement in COVID-19. *EMBO Mol. Med.* **2020**, *12*, No. e12642.
(43) Tanaka, T.; Biancotto, A.; Moaddel, R.; Moore, A. Z.; Gonzalez-Freire, M.; Aon, M. A.; Candia, J.; Zhang, P.; Cheung, F.; Fantoni, G.; Semba, R. D.; Ferrucci, L.; Ferrucci, L. Plasma proteomic signature of age in healthy humans. *Aging Cell* **2018**, *17*, No. e12799.
(44) Nijholt, D. A. T.; Ijsselstijn, L.; van der Weiden, M. M.; Zheng, P.-P.; Sillevis Smitt, P. A. E.; Koudstaal, P. J.; Luider, T. M.; Kros, J. M. Pregnancy Zone Protein is Increased in the Alzheimer's Disease Brain and Associates with Senile Plaques. *J. Alzheimer's Dis.* **2015**, *46*, 227−238.
(45) Jugdutt, B. I.; Sawicki, G. AT1 receptor blockade alters metabolic, functional and structural proteins after reperfused myocardial infarction: detection using proteomics. *Mol. Cell. Biochem.* **2004**, *263*, 179−188.
(46) Fan, Q.-L.; Yang, G.; Liu, X.-D.; Ma, J.-F.; Feng, J.-M.; Jiang, Y.; Wang, L.-N. Effect of losartan on the glomerular protein expression profile of type 2 diabetic KKAy mice. *J. Nephrol.* **2013**, *26*, 517−526.
(47) Abers, M. S.; Delmonte, O. M.; Ricotta, E. E.; Fintzi, J.; Fink, D. L.; de Jesus, A. A. A.; Alehashemi, S.; Oikonomou, V.; Desai, J. V.; Canna, S. W.; Shakoory, B.; Dobbs, K.; Imberti, L.; Sottini, A.; Quiros-Roldan, E.; Castelli, F.; Rossi, C.; Brugnoni, D.; Biondi, A.; Bettini, L. R.; D'Angio', M.; Bonfanti, P.; Castagnoli, R.; Montagna, D.; Licari, A.; Marseglia, G. L.; Gliniewicz, E. F.; Shaw, E.; Kahle, D. E.; Rastegar, A. T.; Stack, M.; Myint-Hpu, K.; Levinson, S. L.; DiNubile, M. J.; Chertow, D. W.; Burbelo, P. D.; Cohen, J. I.; Calvo, K. R.; Tsang, J. S.; Tsang, J. S.; Su, H. C.; Gallin, J. I.; Kuhns, D. B.; Goldbach-Mansky, R.; Lionakis, M. S.; Notarangelo, L. D. An immune-based biomarker signature is associated with mortality in COVID-19 patients. *JCI Insight* **2021**, *6*, No. e144455.
(48) Chen, L.; Long, X.; Xu, Q.; Tan, J.; Wang, G.; Cao, Y.; Wei, J.; Luo, H.; Zhu, H.; Huang, L.; Meng, F.; Huang, L.; Wang, N.; Zhou, X.; Zhao, L.; Chen, X.; Mao, Z.; Chen, C.; Li, Z.; Sun, Z.; Zhao, J.; Wang, D.; Huang, G.; Wang, W.; Zhou, J. Elevated serum levels of S100A8/A9 and HMGB1 at hospital admission are correlated with inferior clinical outcomes in COVID-19 patients. *Cell. Mol. Immunol.* **2020**, *17*, 992−994.
(49) Alkhateeb, T.; Bah, I.; Kumbhare, A.; Youssef, D.; Yao, Z. Q.; McCall, C. E.; Gazzar, M. E. Long Non-Coding RNA Hotairm1 Promotes S100A9 Support of MDSC Expansion during Sepsis. *J. Clin. Cell. Immunol.* **2020**, *11*, 11.
(50) Dubois, C.; Marcé, D.; Faivre, V.; Lukaszewicz, A.-C.; Junot, C.; Fenaille, F.; Simon, S.; Becher, F.; Morel, N.; Payen, D. High

https://doi.org/10.1021/acs.jproteome.1c00863
J. Proteome Res. 2022, 21, 975−992

plasma level of S100A8/S100A9 and S100A12 at admission indicates a higher risk of death in septic shock patients. *Sci. Rep.* **2019**, *9*, 15660.
(51) García, L. F. Immune Response, Inflammation, and the Clinical Spectrum of COVID-19. *Front. Immunol.* **2020**, *11*, 1441.
(52) Thomas, T.; Stefanoni, D.; Dzieciatkowska, M.; Issaian, A.; Nemkov, T.; Hill, R. C.; Francis, R. O.; Hudson, K. E.; Buehler, P. W.; Zimring, J. C.; Hod, E. A.; Hansen, K. C.; Spitalnik, S. L.; D'Alessandro, A. Evidence of Structural Protein Damage and Membrane Lipid Remodeling in Red Blood Cells from COVID-19 Patients. *J. Proteome Res.* **2020**, *19*, 4455−4469.
(53) Moin, A. S. M.; Al-Qaissi, A.; Sathyapalan, T.; Atkin, S. L.; Butler, A. E. Mapping of type 2 diabetes proteins to COVID-19 biomarkers: A proteomic analysis. *Metab. Open* **2021**, *9*, 100074.
(54) Moin, A. S. M.; Sathyapalan, T.; Atkin, S. L.; Butler, A. E. COVID-19 biomarkers for severity mapped to polycystic ovary syndrome. *J. Transl. Med.* **2020**, *18*, 490.
(55) Overmyer, K. A.; Shishkova, E.; Miller, I. J.; Balnis, J.; Bernstein, M. N.; Peters-Clarke, T. M.; Meyer, J. G.; Quan, Q.; Muehlbauer, L. K.; Trujillo, E. A.; He, Y.; Chopra, A.; Chieng, H. C.; Tiwari, A.; Judson, M. A.; Paulson, B.; Brademan, D. R.; Zhu, Y.; Serrano, L. R.; Linke, V.; Drake, L. A.; Adam, A. P.; Schwartz, B. S.; Singer, H. A.; Swanson, S.; Mosher, D. F.; Stewart, R.; Coon, J. J.; Jaitovich, A. Large-Scale Multi-omic Analysis of COVID-19 Severity. *Cell Syst.* **2021**, *12*, 23−40.
(56) Cattaneo, M.; Bertinato, E. M.; Birocchi, S.; Brizio, C.; Malavolta, D.; Manzoni, M.; Muscarella, G.; Orlandi, M. Pulmonary Embolism or Pulmonary Thrombosis in COVID-19? Is the Recommendation to Use High-Dose Heparin for Thromboprophylaxis Justified? *Thromb. Haemostasis* **2020**, *120*, 1230−1232.
(57) Park, J.; Kim, H.; Kim, S. Y.; Kim, Y.; Lee, J.-S.; Dan, K.; Seong, M.-W.; Han, D. In-depth blood proteome profiling analysis revealed distinct functional characteristics of plasma proteins between severe and non-severe COVID-19 patients. *Sci. Rep.* **2020**, *10*, 22418.
(58) Shu, T.; Ning, W.; Wu, D.; Xu, J.; Han, Q.; Huang, M.; Zou, X.; Yang, Q.; Yuan, Y.; Bie, Y.; Pan, S.; Mu, J.; Han, Y.; Yang, X.; Zhou, H.; Li, R.; Ren, Y.; Chen, X.; Yao, S.; Qiu, Y.; Zhang, D.-Y.; Xue, Y.; Shang, Y.; Zhou, X. Plasma Proteomics Identify Biomarkers and Pathogenesis of COVID-19. *Immunity* **2020**, *53*, 1108−1122.
(59) Hoel, H.; Heggelund, L.; Reikvam, D. H.; Stiksrud, B.; Ueland, T.; Michelsen, A. E.; Otterdal, K.; Muller, K. E.; Lind, A.; Muller, F.; Dudman, S.; Aukrust, P.; Dyrhol-Riise, A. M.; Holter, J. C.; Troseid, M. Elevated markers of gut leakage and inflammasome activation in COVID-19 patients with cardiac involvement. *J. Intern. Med.* **2021**, *289*, 523.
(60) Edén, A.; Kanberg, N.; Gostner, J.; Fuchs, D.; Hagberg, L.; Andersson, L. M.; Lindh, M.; Price, R. W.; Zetterberg, H.; Gisslén, M. CSF Biomarkers in Patients With COVID-19 and Neurologic Symptoms: A Case Series. *Neurology* **2021**, *96*, e294−e300.
(61) Kimhofer, T.; Lodge, S.; Whiley, L.; Gray, N.; Loo, R. L.; Lawler, N. G.; Nitschke, P.; Bong, S.-H.; Morrison, D. L.; Begum, S.; Richards, T.; Yeap, B. B.; Smith, C.; Smith, K. G. C.; Holmes, E.; Nicholson, J. K. Integrative Modeling of Quantitative Plasma Lipoprotein, Metabolic, and Amino Acid Data Reveals a Multiorgan Pathological Signature of SARS-CoV-2 Infection. *J. Proteome Res.* **2020**, *19*, 4442−4454.
(62) Morris, D. C.; Jaehne, A. K.; Chopp, M.; Zhang, Z.; Poisson, L.; Chen, Y.; Datta, I.; Rivers, E. P. Proteomic Profiles of Exosomes of Septic Patients Presenting to the Emergency Department Compared to Healthy Controls. *J. Clin. Med.* **2020**, *9*, 2930.
(63) Garcia-Obregon, S.; Azkargorta, M.; Seijas, I.; Pilar-Orive, J.; Borrego, F.; Elortza, F.; Boyano, M. D.; Astigarraga, I. Identification of a panel of serum protein markers in early stage of sepsis and its validation in a cohort of patients. *J. Microbiol. Immunol. Infect.* **2018**, *51*, 465−472.
(64) Jang, S.; Jang, W. Y.; Choi, M.; Lee, J.; Kwon, W.; Yi, J.; Park, S. J.; Yoon, D.; Lee, S.; Kim, M. O.; Ryoo, Z. Y. Serum amyloid A1 is involved in amyloid plaque aggregation and memory decline in amyloid beta abundant condition. *Transgenic Res.* **2019**, *28*, 499−508.
(65) Huang, C.; Huang, L.; Wang, Y.; Li, X.; Ren, L.; Gu, X.; Kang, L.; Guo, L.; Liu, M.; Zhou, X.; Luo, J.; Huang, Z.; Tu, S.; Zhao, Y.; Chen, L.; Xu, D.; Li, Y.; Li, C.; Peng, L.; Li, Y.; Xie, W.; Cui, D.; Shang, L.; Fan, G.; Xu, J.; Wang, G.; Wang, Y.; Zhong, J.; Wang, C.; Wang, J.; Zhang, D.; Cao, B. 6-month consequences of COVID-19 in patients discharged from hospital: a cohort study. *Lancet* **2021**, *397*, 220.
(66) Cheng, Z.; Yin, J.; Yuan, H.; Jin, C.; Zhang, F.; Wang, Z.; Liu, X.; Wu, Y.; Wang, T.; Xiao, S. Blood-Derived Plasma Protein Biomarkers for Alzheimer's Disease in Han Chinese. *Front. Aging Neurosci.* **2018**, *10*, 414.
(67) Hondius, D. C.; Eigenhuis, K. N.; Morrema, T. H. J.; van der Schors, R. C.; van Nierop, P.; Bugiani, M.; Li, K. W.; Hoozemans, J. J. M.; Smit, A. B.; Rozemuller, A. J. M. Proteomics analysis identifies new markers associated with capillary cerebral amyloid angiopathy in Alzheimer's disease. *Acta Neuropathol. Commun.* **2018**, *6*, 46.
(68) Pepys, M. B.; Herbert, J.; Hutchinson, W. L.; Tennent, G. A.; Lachmann, H. J.; Gallimore, J. R.; Lovat, L. B.; Bartfai, T.; Alanine, A.; Hertel, C.; Hoffmann, T.; Jakob-Roetne, R.; Norcross, R. D.; Kemp, J. A.; Yamamura, K.; Suzuki, M.; Taylor, G. W.; Murray, S.; Thompson, D.; Purvis, A.; Kolstoe, S.; Wood, S. P.; Hawkins, P. N. Targeted pharmacological depletion of serum amyloid P component for treatment of human amyloidosis. *Nature* **2002**, *417*, 254−259.
(69) Al-Shawi, R.; Tennent, G. A.; Millar, D. J.; Richard-Londt, A.; Brandner, S.; Werring, D. J.; Simons, J. P.; Pepys, M. B. Pharmacological removal of serum amyloid P component from intracerebral plaques and cerebrovascular Abeta amyloid deposits in vivo. *Open Biol.* **2016**, *6*, 150202.
(70) Iacob, E.; Light, K. C.; Tadler, S. C.; Weeks, H. R.; White, A. T.; Hughen, R. W.; Vanhaitsma, T. A.; Bushnell, L.; Light, A. R. Dysregulation of leukocyte gene expression in women with medication-refractory depression versus healthy non-depressed controls. *BMC Psychiatr.* **2013**, *13*, 273.
(71) Strunz, M.; Jarrell, J. T.; Cohen, D. S.; Rosin, E. R.; Vanderburg, C. R.; Huang, X. Modulation of SPARC/Hevin Proteins in Alzheimer's Disease Brain Injury. *J. Alzheimer's Dis.* **2019**, *68*, 695−710.
(72) Campolongo, M.; Benedetti, L.; Podhajcer, O. L.; Pitossi, F.; Depino, A. M. Hippocampal SPARC regulates depression-related behavior. *Gene Brain Behav.* **2012**, *11*, 966−976.
(73) Jiang, Y.; Rosborough, B. R.; Chen, J.; Das, S.; Kitsios, G. D.; McVerry, B. J.; Mallampalli, R. K.; Lee, J. S.; Ray, A.; Chen, W.; Ray, P. Single cell RNA sequencing identifies an early monocyte gene signature in acute respiratory distress syndrome. *JCI Insight* **2020**, *5*, No. e135678.
(74) Mossel, D. M.; Moganti, K.; Riabov, V.; Weiss, C.; Kopf, S.; Cordero, J.; Dobreva, G.; Rots, M. G.; Klüter, H.; Harmsen, M. C.; Kzhyshkowska, J. Epigenetic Regulation of S100A9 and S100A12 Expression in Monocyte-Macrophage System in Hyperglycemic Conditions. *Front. Immunol.* **2020**, *11*, 1071.
(75) Carr, S. A.; Abbatiello, S. E.; Ackermann, B. L.; Borchers, C.; Domon, B.; Deutsch, E. W.; Grant, R. P.; Hoofnagle, A. N.; Hüttenhain, R.; Koomen, J. M.; Liebler, D. C.; Liu, T.; MacLean, B.; Mani, D.; Mansfield, E.; Neubert, H.; Paulovich, A. G.; Reiter, L.; Vitek, O.; Aebersold, R.; Anderson, L.; Bethem, R.; Blonder, J.; Boja, E.; Botelho, J.; Boyne, M.; Bradshaw, R. A.; Burlingame, A. L.; Chan, D.; Keshishian, H.; Kuhn, E.; Kinsinger, C.; Lee, J. S. H.; Lee, S.-W.; Moritz, R.; Oses-Prieto, J.; Rifai, N.; Ritchie, J.; Rodriguez, H.; Srinivas, P. R.; Townsend, R. R.; Van Eyk, J.; Whiteley, G.; Wiita, A.; Weintraub, S. Targeted peptide measurements in biology and medicine: best practices for mass spectrometry-based assay development using a fit-for-purpose approach. *Mol. Cell. Proteomics* **2014**, *13*, 907−917.
(76) Huang, C.-H.; Kuo, C.-J.; Liang, S.-S.; Chi, S.-W.; Hsi, E.; Chen, C.-C.; Lee, K.-T.; Chiou, S.-H. Onco-proteogenomics identifies urinary S100A9 and GRN as potential combinatorial biomarkers for early diagnosis of hepatocellular carcinoma. *BBA Clin.* **2015**, *3*, 205−213.

https://doi.org/10.1021/acs.jproteome.1c00863
J. Proteome Res. 2022, 21, 975−992

(77) Caseiro, A.; Ferreira, R.; Padrão, A.; Quintaneiro, C.; Pereira, A.; Marinheiro, R.; Vitorino, R.; Amado, F. Salivary proteome and peptidome profiling in type 1 diabetes mellitus using a quantitative approach. *J. Proteome Res.* **2013**, *12*, 1700−1709.
(78) Xu, D.; Li, Y.; Li, X.; Wei, L.-L.; Pan, Z.; Jiang, T.-T.; Chen, Z.-L.; Wang, C.; Cao, W.-M.; Zhang, X.; Ping, Z.-P.; Liu, C.-M.; Liu, J.-Y.; Li, Z.-J.; Li, J.-C. Serum protein S100A9, SOD3, and MMP9 as new diagnostic biomarkers for pulmonary tuberculosis by iTRAQ-coupled two-dimensional LC-MS/MS. *Proteomics* **2015**, *15*, 58−67.
(79) Luther, T.; Bülow-Anderberg, S.; Larsson, A.; Rubertsson, S.; Lipcsey, M.; Frithiof, R.; Hultström, M. COVID-19 patients in intensive care develop predominantly oliguric acute kidney injury. *Acta Anaesthesiol. Scand.* **2021**, *65*, 364−372.
(80) Bedet, A.; Razazi, K.; Boissier, F.; Surenaud, M.; Hue, S.; Giraudier, S.; Brun-Buisson, C.; Mekontso Dessap, A. Mechanisms of Thrombocytopenia During Septic Shock: A Multiplex Cluster Analysis of Endogenous Sepsis Mediators. *Shock* **2018**, *49*, 641−648.
(81) Iba, T.; Connors, J. M.; Levy, J. H. The coagulopathy, endotheliopathy, and vasculitis of COVID-19. *Inflamm. Res.* **2020**, *69*, 1181−1189.
(82) Colling, M. E.; Kanthi, Y. COVID-19-associated coagulopathy: An exploration of mechanisms. *Vasc. Med.* **2020**, *25*, 471−478.
(83) Magro, C.; Mulvey, J. J.; Berlin, D.; Nuovo, G.; Salvatore, S.; Harp, J.; Baxter-Stoltzfus, A.; Laurence, J. Complement associated microvascular injury and thrombosis in the pathogenesis of severe COVID-19 infection: A report of five cases. *Transl. Res.* **2020**, *220*, 1−13.
(84) Zolfaghari Emameh, R.; Falak, R.; Bahreini, E. Application of System Biology to Explore the Association of Neprilysin, Angiotensin-Converting Enzyme 2 (ACE2), and Carbonic Anhydrase (CA) in Pathogenesis of SARS-CoV-2. *Biol. Proced. Online* **2020**, *22*, 11.
(85) Wang, J.; Guo, S.; Zhang, Y.; Gao, K.; Zuo, J.; Tan, N.; Du, K.; Ma, Y.; Hou, Y.; Li, Q.; Xu, H.; Huang, J.; Huang, Q.; Na, H.; Wang, J.; Wang, X.; Xiao, Y.; Zhu, J.; Chen, H.; Liu, Z.; Wang, M.; Zhang, L.; Wang, W. Clinical features and risk factors for severe inpatients with COVID-19: A retrospective study in China. *PLoS One* **2020**, *15*, No. e0244125.
(86) Ouyang, S.-M.; Zhu, H.-Q.; Xie, Y.-N.; Zou, Z.-S.; Zuo, H.-M.; Rao, Y.-W.; Liu, X.-Y.; Zhong, B.; Chen, X. Temporal changes in laboratory markers of survivors and non-survivors of adult inpatients with COVID-19. *BMC Infect. Dis.* **2020**, *20*, 952.
(87) Li, Y.; Yang, S.; Peng, D.; Zhu, H.-M.; Li, B.-Y.; Yang, X.; Sun, X.-L.; Zhang, M. Predictive value of serum cystatin C for risk of mortality in severe and critically ill patients with COVID-19. *World J. Clin. Cases* **2020**, *8*, 4726−4734.
(88) Petito, E.; Falcinelli, E.; Paliani, U.; Cesari, E.; Vaudo, G.; Sebastiano, M.; Cerotto, V.; Guglielmini, G.; Gori, F.; Malvestiti, M.; Becattini, C.; Paciullo, F.; De Robertis, E.; Bury, L.; Lazzarini, T.; Gresele, P.; investigators, C. s. Neutrophil more than platelet activation associates with thrombotic complications in COVID-19 patients. *J. Infect. Dis.* **2021**, *223* (6), 933−944.
(89) Zinter, M. S.; Delucchi, K. L.; Kong, M. Y.; Orwoll, B. E.; Spicer, A. S.; Lim, M. J.; Alkhouli, M. F.; Ratiu, A. E.; McKenzie, A. V.; McQuillen, P. S.; Dvorak, C. C.; Calfee, C. S.; Matthay, M. A.; Sapru, A. Early Plasma Matrix Metalloproteinase Profiles. A Novel Pathway in Pediatric Acute Respiratory Distress Syndrome. *Am. J. Respir. Crit. Care Med.* **2019**, *199*, 181−189.
(90) Varim, C.; Demirci, T.; Cengiz, H.; Hacibekiroglu, I.; Tuncer, F. B.; Cokluk, E.; Toptan, H.; Karabay, O.; Yildirim, I. *Relationship between Serum Osteopontin Levels and the Severity of COVID-19 Infection*; Wien Klin Wochenschr, 2020.
(91) Adu-Agyeiwaah, Y.; Grant, M. B.; Obukhov, A. G. The Potential Role of Osteopontin and Furin in Worsening Disease Outcomes in COVID-19 Patients with Pre-Existing Diabetes. *Cells* **2020**, *9*, 2528.
(92) Tong, M.; Jiang, Y.; Xia, D.; Xiong, Y.; Zheng, Q.; Chen, F.; Zou, L.; Xiao, W.; Zhu, Y. Elevated Expression of Serum Endothelial Cell Adhesion Molecules in COVID-19 Patients. *J. Infect. Dis.* **2020**, *222*, 894−898.
(93) Fang, Y.; Li, C.; Shao, R.; Yu, H.; Zhang, Q. The role of biomarkers of endothelial activation in predicting morbidity and mortality in patients with severe sepsis and septic shock in intensive care: A prospective observational study. *Thromb. Res.* **2018**, *171*, 149−154.
(94) Mosevoll, K. A.; Skrede, S.; Markussen, D. L.; Fanebust, H. R.; Flaatten, H. K.; Assmus, J.; Reikvam, H.; Bruserud, Ø. Inflammatory Mediator Profiles Differ in Sepsis Patients With and Without Bacteremia. *Front. Immunol.* **2018**, *9*, 691.
(95) Amalakuhan, B.; Habib, S. A.; Mangat, M.; Reyes, L. F.; Rodriguez, A. H.; Hinojosa, C. A.; Soni, N. J.; Gilley, R. P.; Bustamante, C. A.; Anzueto, A.; Levine, S. M.; Peters, J. I.; Aliberti, S.; Sibila, O.; Chalmers, J. D.; Torres, A.; Waterer, G. W.; Martin-Loeches, I.; Bordon, J.; Blanquer, J.; Sanz, F.; Marcos, P. J.; Rello, J.; Ramirez, J.; Solé-Violán, J.; Luna, C. M.; Feldman, C.; Witzenrath, M.; Wunderink, R. G.; Stolz, D.; Wiemken, T. L.; Shindo, Y.; Dela Cruz, C. S.; Orihuela, C. J.; Restrepo, M. I. Endothelial adhesion molecules and multiple organ failure in patients with severe sepsis. *Cytokine* **2016**, *88*, 267−273.
(96) Ward, S. E.; Curley, G. F.; Lavin, M.; Fogarty, H.; Karampini, E.; McEvoy, N. L.; Clarke, J.; Boylan, M.; Alalqam, R.; Worrall, A. P.; Kelly, C.; Barra, E.; Glavey, S.; Ni Cheallaigh, C.; Bergin, C.; Martin-Loeches, I.; Townsend, L.; Mallon, P. W.; O'Sullivan, J. M.; O'Donnell, J. S.; O'Connell, N.; Ryan, K.; Byrne, M.; Preston, R.; Kenny, D. Von Willebrand factor propeptide in severe coronavirus disease 2019 (COVID-19): evidence of acute and sustained endothelial cell activation. *Br. J. Haematol.* **2021**, *192*, 714−719.
(97) Fan, B. E.; Ng, J.; Chan, S. S. W.; Christopher, D.; Tso, A. C. Y.; Ling, L. M.; Young, B. E.; Wong, L. J. L.; Sum, C. L. L.; Tan, H. T.; Ang, M. K.; Lim, G. H.; Ong, K. H.; Kuperan, P.; Chia, Y. W. COVID-19 associated coagulopathy in critically ill patients: A hypercoagulable state demonstrated by parameters of haemostasis and clot waveform analysis. *J. Thromb. Thrombolysis* **2021**, *51*, 663.
(98) Ladikou, E. E.; Sivaloganathan, H.; Milne, K. M.; Arter, W. E.; Ramasamy, R.; Saad, R.; Stoneham, S. M.; Philips, B.; Eziefula, A. C.; Chevassut, T. Von Willebrand factor (vWF): marker of endothelial damage and thrombotic risk in COVID-19? *Clin. Med.* **2020**, *20*, e178−e182.
(99) Henry, B. M.; Benoit, S. W.; de Oliveira, M. H. S.; Lippi, G.; Favaloro, E. J.; Benoit, J. L. ADAMTS13 activity to von Willebrand factor antigen ratio predicts acute kidney injury in patients with COVID-19: Evidence of SARS-CoV-2 induced secondary thrombotic microangiopathy. *Int. J. Lab. Hematol.* **2021**, *43*, 129.

https://doi.org/10.1021/acs.jproteome.1c00863
J. Proteome Res. 2022, 21, 975−992